Available online at www.sciencedirect.com
SCIENCE DIRECT®
Developmental Biology 267 (2004) 320–341
DEVELOPMENTAL BIOLOGY
www.elsevier.com/locate/ydbio

bullwinkle is required for epithelial morphogenesis during *Drosophila* oogenesis☆

Jennie B. Dorman,[a,b] Karen E. James,[a] Scott E. Fraser,[c] Daniel P. Kiehart,[d] and Celeste A. Berg[a,b,*]

[a] *Department of Genome Sciences, University of Washington, Seattle, WA 98195-7730, USA*
[b] *Molecular and Cellular Biology Program, University of Washington, Seattle, WA 98195-7275, USA*
[c] *Biology Division, Caltech, Beckman Institute 139-74, Pasadena, CA 91125, USA*
[d] *Developmental, Cell and Molecular Biology Group, Department of Biology, Duke University, Durham, NC 27708-1000, USA*

Received for publication 29 July 2003, revised 4 October 2003, accepted 7 October 2003

Abstract

Many organs, such as the liver, neural tube, and lung, form by the precise remodeling of flat epithelial sheets into tubes. Here we investigate epithelial tubulogenesis in *Drosophila melanogaster* by examining the development of the dorsal respiratory appendages of the eggshell. We employ a culture system that permits confocal analysis of stage 10–14 egg chambers. Time-lapse imaging of GFP-Moesin-expressing egg chambers reveals three phases of morphogenesis: tube formation, anterior extension, and paddle maturation. The dorsal-appendage-forming cells, previously thought to represent a single cell fate, consist of two subpopulations, those forming the tube roof and those forming the tube floor. These two cell types exhibit distinct morphological and molecular features. Roof-forming cells constrict apically and express high levels of Broad protein. Floor cells lack Broad, express the *rhomboid-lacZ* marker, and form the floor by directed cell elongation. We examine the morphogenetic phenotype of the *bullwinkle* (*bwk*) mutant and identify defects in both roof and floor formation. Dorsal appendage formation is an excellent system in which cell biological, molecular, and genetic tools facilitate the study of epithelial morphogenesis.

Keywords: Epithelial morphogenesis; Eggshell; Dorsal appendage; Tubulogenesis; Oogenesis; *Drosophila*; Moesin; Culture; Patterning; EGFR

Introduction

Epithelial morphogenesis is the means by which flat sheets of cells transform into more complex shapes. This process occurs widely throughout animal development and is essential to the construction of the body. Epithelial morphogenesis drives early fundamental developmental events such as gastrulation and neurulation and is vital for the later formation of virtually all organs, including the skin, respiratory system, mammary glands, and digestive, urinary, and reproductive tracts (Fristrom, 1988; Kolega, 1986; von Kalm et al., 1995).

During morphogenesis, flat epithelial sheets remodel into many different shapes, including pockets, spheres, and tubes. Epithelial tubulogenesis has been studied in many organisms and entails diverse mechanisms such as budding, wrapping, and cavitation (Hogan and Kolodziej, 2002; Lubarsky and Krasnow, 2003). Nonetheless, many questions remain about the regulation and execution of epithelial tubulogenesis. How, for example, are the actions of cells forming different parts of the tube coordinated, and how is tube elongation accomplished? These questions may be addressed by investigating the behavior of cells that secrete the dorsal appendages, specialized respiratory structures of the *Drosophila melanogaster* eggshell (Hinton, 1969; Spradling, 1993). Each dorsal appendage consists of a long cylindrical stalk of highly porous chorion proteins with a flattened plastron (or "paddle") at the tip, which is thought to function as a gill when the egg chamber is submerged in water or rotting fruit (Hinton, 1969; Margaritis et al., 1980; Spradling, 1993).

☆ Supplementary data associated with this article may be found, in the online version, at doi:10.1016/j.ydbio.2003.10.020.

* Corresponding author. Department of Genome Sciences, University of Washington, Box 357730, Seattle, WA 98195-7730. Fax: +1-206-543-0754.
E-mail address: berg@gs.washington.edu (C.A. Berg).

0012-1606/$ - see front matter © 2003 Elsevier Inc. All rights reserved.
doi:10.1016/j.ydbio.2003.10.020

To create the two dorsal appendages, two groups of cells in the egg chamber reorganize and change shape, altering from flat sheets into tubes. The dorsal-appendage-forming cells then secrete eggshell proteins into the tube lumens. During eggshell maturation, these chorion proteins are cross-linked; the dorsal-appendage-forming cells slough off, revealing the chorionic dorsal appendages inside (Spradling, 1993). Although the dorsal appendages are themselves acellular accumulations of chorion proteins on the eggshell, their morphology reflects the successful tubulogenesis of the cells that secreted them. Thus, dorsal appendage morphogenesis can serve as a simple model of epithelial tubulogenesis coupled with secretion, and therefore may shed light on the processes of kidney, liver, and breast development.

A number of technical advantages facilitate our studies of epithelial morphogenesis in this tissue. Synthesis of the dorsal appendages occurs rapidly during the last 10 h of oogenesis (Spradling, 1993). Unlike many other instances of epithelial morphogenesis, dorsal appendage formation takes place without the complicating factors of cell division and cell death (King, 1970; King and Vanoucek, 1960; Nezis et al., 2002). Instead, it relies exclusively on cell-shape changes and movement, allowing us to focus on these essential aspects of epithelial morphogenesis. The dorsal-appendage-forming cells reside in an optically accessible location above the opaque yolk of the oocyte, allowing detailed image analysis by confocal microscopy. Furthermore, mutants with defective dorsal appendages provide insight into the mechanisms governing this morphogenetic process. Finally, sophisticated genetic studies have set the stage for analyses of dorsal appendage morphogenesis by illuminating the process by which the fate of the dorsal appendage-forming cells is initially determined (reviewed by Dobens and Raftery, 2000; Nilson and Schüpbach, 1999; Stevens, 1998).

The patterning of the dorsal appendage-forming cells requires extensive communication between different cell types of the egg chamber. The egg chamber is composed of 16 interconnected germline cells—a single oocyte (Oo) and 15 support cells called nurse cells (NCs)—which are ensheathed by a layer of approximately 650 somatic cells called follicle cells (Fig. 1G; Margolis and Spradling, 1995; Spradling, 1993). At the start of morphogenesis in stage 10B, the nurse cells occupy the anterior half of the egg chamber and are enclosed by a thin squamous epithelium of follicle cells called stretch cells (SCs; Figs. 1A and G′, not shown in A′and G). The oocyte, which occupies the posterior half of the egg chamber, is covered by an epithelial sheet of columnar-shaped follicle cells (Fig. 1G). Signaling between and within these cell layers specifies two dorsal appendage primordia (Wasserman and Freeman, 1998).

The positions of the bilaterally symmetric dorsal appendage primordia are asymmetric with respect to both the D-V and the A-P axes and are established by the convergence of two signaling pathways. The diffusible signal DPP (a BMP2/4 homolog in the TGF-β superfamily) emanates from the stretch cells anterior to the columnar epithelium and confers anterior fate (Deng and Bownes, 1997; Dobens and Raftery, 2000; Peri and Roth, 2000; Twombly et al., 1996). A second signal, the TGF-α homolog Gurken (GRK), is localized at the dorsal anterior corner of the oocyte and acts via the EGF-Receptor (EGFR) pathway to confer dorsal fate in the overlying follicle cells (reviewed in Nilson and Schüpbach, 1999). These two signals overlap in a saddle-shaped zone at the dorsal anterior of the columnar epithelium. Next, feedback inhibition of EGFR signaling by Argos along the dorsal midline bisects the saddle-shaped zone into two primordia (Peri et al., 1999; Wasserman and Freeman, 1998). By stage 10B, the combined actions of these molecules establish two dorsal appendage primordia near the anterior margin of the columnar follicular epithelium, one on either side of the dorsal midline (Fig. 1A).

Despite the wealth of information concerning the specification of dorsal appendage cell fate, relatively little is known about the subsequent morphogenetic process. Appendage-patterning studies often emphasize early signaling events and eggshell endpoints but explore the intervening morphogenetic events in much less detail. In addition, many of the molecules required for dorsal appendage formation play a role during patterning, obscuring any possible function in morphogenesis.

Molecules that may function during epithelial morphogenesis in the egg chamber include certain cytoskeletal and adhesion proteins and their regulators. The homophilic cell-adhesion protein E-cadherin (ECAD) is required in the follicular epithelium for border- and centripetal-cell migration and may act in dorsal appendage formation as well (Niewiadomska et al., 1999). Large follicle-cell clones lacking β_{PS} integrin result in abnormal dorsal appendages, revealing a requirement for this class of cell-adhesion molecule (Duffy et al., 1998). Mutations in genes that encode cytoskeletal elements such as nonmuscle myosin subunits, profilin, and villin produce aberrant dorsal appendages, although the latter two may affect morphogenesis via their role in patterning (Edwards and Kiehart, 1996; Mahajan-Miklos and Cooley, 1994b; Manseau et al., 1996). Candidate regulators of dorsal appendage morphogenesis include the transcription factors Broad (Deng and Bownes, 1997) and Tramtrack-69 (French et al., 2003) and components of the Jun-*N*-terminal kinase (JNK) pathway (Dequier et al., 2001; Dobens et al., 2001; Suzanne et al., 2001).

Only a few brief descriptions of dorsal appendage morphogenesis exist in the literature (King, 1970; reviewed in Dobens and Raftery, 2000; Spradling, 1993; Waring, 2000). Many studies of late oogenesis have focused on other processes that occur concomitantly with dorsal appendage formation, such as nurse-cell ‘dumping’ and centripetal-cell migration. Starting in late stage 10B or early stage 11, the nurse cells undergo a programmed cell death process that begins with the rapid transfer or ‘dumping’ of their contents into the oocyte, which expands reciprocally (Mahajan-Miklos and Cooley, 1994a). At the same time,

centripetal cells (cen), a subset of columnar follicle cells just anterior to the dorsal appendage primordia, move between the oocyte and the degenerating nurse cells (Fig. 1H) to seal off the anterior face of the oocyte. These cells form the anterior-most portion of the eggshell, called the operculum (Edwards and Kiehart, 1996; Spradling, 1993). They collaborate with the border cells to form the micropyle, a hole for sperm entry (King, 1970; Margaritis, 1984; Montell et al., 1992). While distinct from dorsal appendage formation, these processes influence the morphogenetic environment in which dorsal appendage formation takes place.

Morphogenetic analyses establish a framework for understanding the mechanisms governing normal developmental processes and provide vital context for interpreting the effects of genetic mutations and teratogenic agents. Here, we provide a detailed morphogenetic analysis of dorsal appendage formation using three complementary approaches. First, we directly observe the shape changes and movements of the dorsal-appendage-forming cells during wild-type morphogenesis using a GFP-Moesin fusion protein expressed throughout the follicular epithelia of cultured egg chambers. Second, we examine fixed tissue and correlate the cell-shape changes and movements observed in cultured egg chambers with the expression of molecular markers that identify the cells' patterning histories, allowing us to define an important link between patterning and the specific events of morphogenesis. Lastly, we employ these molecular and imaging tools to examine morphogenetic phenotypes in the *bullwinkle* (*bwk*) mutant, which patterns the dorsal appendage primordia normally but produces egg chambers with moose-antler-shaped dorsal appendages (Rittenhouse and Berg, 1995). *bullwinkle* encodes an HMG-box containing putative transcription factor with homologues in human, mouse, nematode, and yeast (Rittenhouse, 1996; Berg et al., unpublished results). Furthermore, *bwk* acts in the germline and regulates morphogenesis via a signaling pathway that is independent of the known TGF-α, EGFR-dependent process (Rittenhouse and Berg, 1995). As such, it represents an excellent opportunity to investigate the mechanisms and regulation of morphogenesis.

Materials and methods

Fly stocks

For the culture studies, we employed GAL4 CY2 (Queenan et al., 1997) to drive expression of UAS-GFP-Moesin (UAS-GMA; Bloor and Kiehart, 2001) throughout the follicular epithelium. The wild-type genotype was w^{1118} *UAS-GMA/*w^{1118}; *GAL4 CY2/+*; and the genotype for *bullwinkle* flies was w^{1118} *UAS-GMA/*w^{1118}; *GAL4 CY2/+*; ry^{506} *cv-c sbd* bwk^{151}/ry^{506} *cv-c sbd* bwk^{8482}. Both *bwk* alleles are hypomorphic mutations that produce strong dorsal appendage defects (Rittenhouse and Berg, 1995).

For studies of roof and floor formation in fixed egg chambers, we used flies bearing a 2.2-kb fragment of the

Fig. 1. Schematic diagrams depicting dorsal appendage morphogenesis in wild-type *D. melanogaster* egg chambers. Time proceeds down the page from stage 10B (top row) to stage 14 (bottom row). Stages 10B and 14 views show the entire egg chamber, with boxes around the dorsal appendage-forming cells. Stages 11–13 images show close-up views of the cells forming a single appendage. The four columns depict different views of each time point: *Column I* features dorsal views of the roof cells (blue) overlying floor cells (red) of the left appendage. This column depicts the changing shape and configuration of the apically constricted roof cells (blue). Anterior is to the left. The dorsal midline is indicated by the white line in stage 10B panels and is located at the top of stages 11–13 panels. (A) The box highlights cells in the left dorsal appendage primordium. Stretch cells (SC, green), which cover the nurse cells (NCs, purple), are here cut away to reveal the nurse cells. (B–E) Some of the roof cell bodies have been removed to reveal the shapes of the roof cell apices (apical footprint of entire roof population is shown in grey, bordered by dashed white line). (B) In early stage 11, all roof cell apices are constricted and form an almond-shaped array (inside dashed white line). (C) By late stage 11, the roof cell apices constrict twofold more and adopt a short triangular array. (D) The roof cell population lengthens during anterior extension. (E) Roof cells expand their apices and flatten during paddle maturation. (F) Stage 14 egg chamber before follicle cell sloughing shows roof cells in stalk (S) and paddle (P) regions. Box shows area depicted in (E). For a view of the stage 14 eggshell, see Fig. 8D. *Column II* reveals floor cell (red) morphology by removing the roof cells. The orientation is identical to column I. (A′) The box highlights floor cells (red) in the left dorsal appendage primordium. (B′–E′) To reveal the floor cell morphology, overlying roof cells have been removed. However, the apical footprint of the roof population (inside dashed blue line) is provided for comparison with column I. During late elongation, the anterior row of floor cells initiates elongation (arrow, B′), followed by the medial row (arrow, C′). This elongation continues until floor cells from the anterior and medial rows meet and seal together (D′). Floor cells cease elongation and shorten to create the mature paddle shape (E′). Box in F′ indicates area shown in E′. *Column III* displays longitudinal sections showing tube formation of cells that secrete the dorsal appendages. Anterior is to the left and dorsal is at the top. The stretch cells, which overly the nurse cells at all stages, are not shown. The location of each longitudinal section is indicated by grey lines on the equivalent roof and floor views. (G) Dorsal-appendage-forming cells (blue and red) have already undergone early elongation relative to ventral cells. Box highlights area shown in H. (H) Roof cells (blue) constrict their apices (a); basal surfaces (b) remain unconstricted and hexagonal. (I) Floor cells (red) drop their nuclei and elongate underneath the roof to form the bottom surface of the tube. (J) Dorsal-appendage-forming cells extend anteriorly over the degenerating nurse cells; a small white chorion-filled lumen (black arrow) is visible. (K) Roof cells unconstrict their apices and flatten during paddle formation as the chorion (white) thickens. (L) A dorsal view of a stage 14 egg chamber displays a longitudinal section of the mature tube. The paddle is oriented perpendicular to the page. *Column IV* shows partial cross sections of the egg chamber and features the cells forming both left and right appendages. Anterior is at the top left, pointing into the page. The location of each cross section is indicated by green lines on the equivalent roof and floor views. (H′–I′) Floor cells (red) from the medial row drop down underneath the apically constricted roof cells (blue). (J′) Floor cells become very thin as a result of their significant elongation; small chorion-filled lumens are visible (white). The stretch cells, which separate the floor cells from the nurse cells, are not shown here or in subsequent panels. (K′) Cross section of paddle during maturation when roof cells flatten. (L′) Stage 14 egg chamber depicts orientation of cross section in K′. *Key to colors and abbreviations*: a = apical; anterior = anterior row of floor cells; b = basal; c = chorion (white space in longitudinal and cross sections); cen = centripetal cells (light blue); dorsal midline (white line on stage 10B roof and floor views); main body follicle cells (light blue); medial = medial row of floor cells; Oo = Oocyte (yellow); gv = germinal vesicle (= oocyte nucleus; brown); NCs = nurse cells (purple); P = paddle; S = stalk; SC = stretch cells (green, cut away to reveal NCs, not shown in stages 11–14).

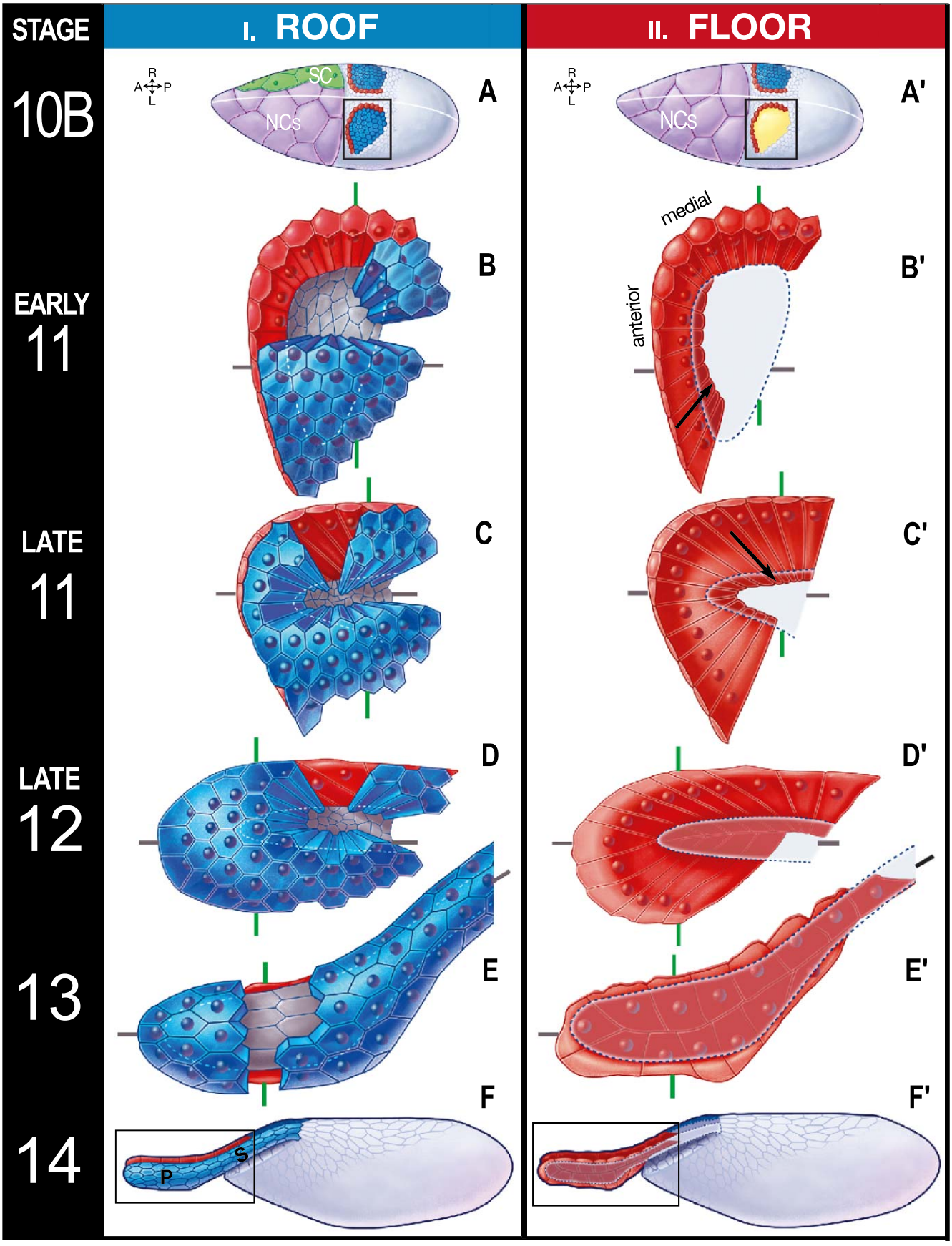
STAGE
I. ROOF
II. FLOOR
10B
EARLY 11
LATE 11
LATE 12
13
14
R
A
P
L
SC
NCs
A
A'
B
B'
medial
anterior
C
C'
D
D'
E
E'
F
F'
S
P

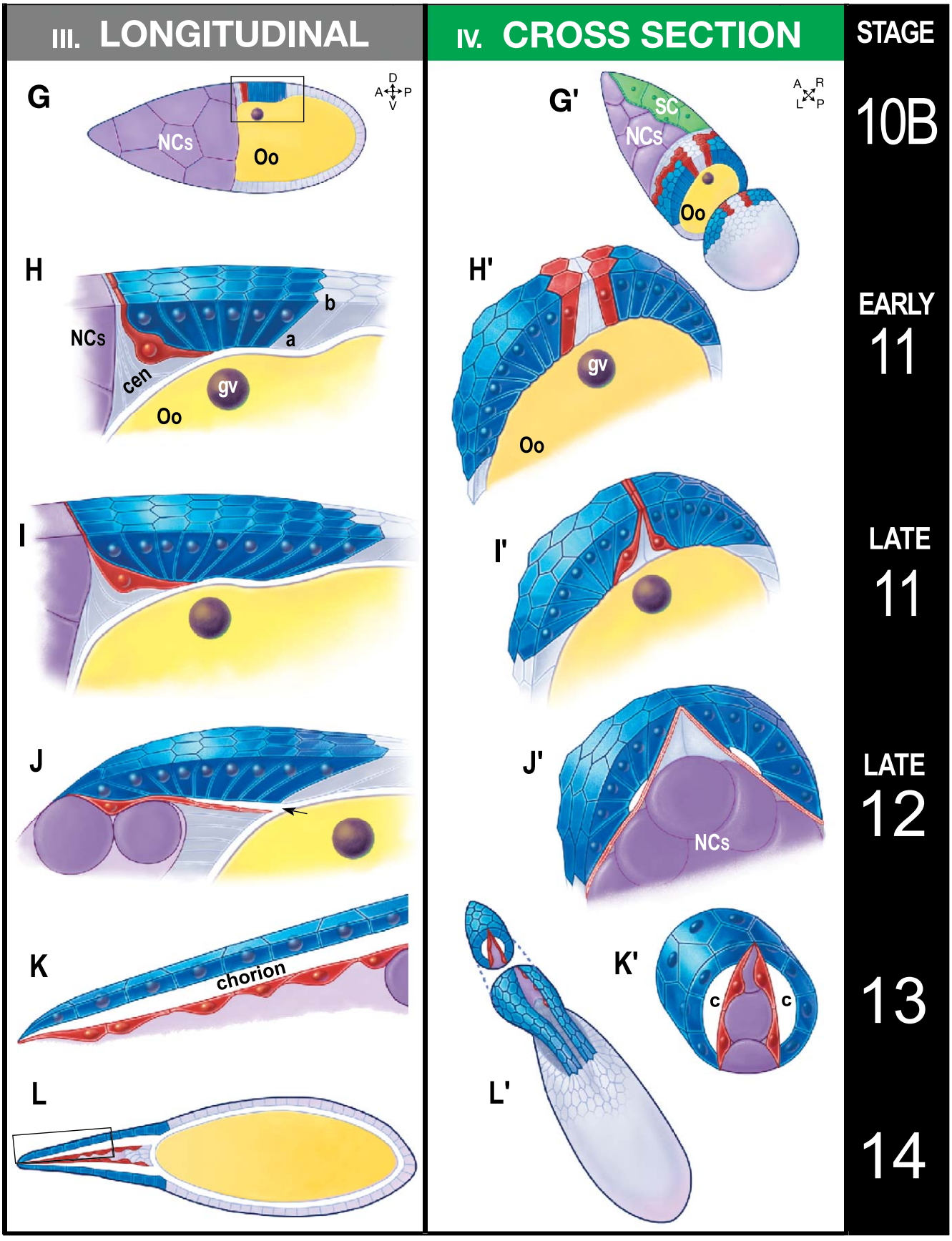

Fig. 1 (*continued*).

rhomboid-1 promoter fused to *lacZ* (rho-lacZ R1.1 line, Ip et al., 1992). While females homozygous for *rho-lacZ* lay a small proportion of ventralized eggs, heterozygotes produce egg chambers with wild-type dorsal appendages; heterozygotes were used for studies of fixed wild-type egg chambers unless otherwise noted. Since null *bullwinkle* mutants die as larvae, we examined egg chambers produced by females bearing a *P*-element-induced hypomorphic allele, bwk^{151}, in trans to a deficiency, $bwk^{\Delta 11}$ (Rittenhouse and Berg, 1995), and also carrying the *rho-lacZ* marker (full genotype: *w*; ry^{506} *cv-c sbd* bwk^{151}/ry^{506} $bwk^{\Delta 11}$ *e P*[*w*+; *rho-lacZ-R*1.1]).

Notes on the rho-lacZ marker

The majority of the floor cells express *rho-lacZ,* but some do not due to variability of marker expression (diamonds, Figs. 4C and G). The position of these gaps in β-Gal staining is random from one egg chamber to the next and thus is not likely to be significant. While this variability complicates the analysis in certain respects, it also produces clear cell boundaries, revealing cell morphology more distinctly than if all the cells stained uniformly. Furthermore, floor cells that lack cytoplasmic β-Gal expression usually exhibit nuclear staining (arrowhead, Fig. 3E). Even floor cells that totally lack *rho-lacZ* expression (diamonds, Fig. 4C) may be recognized based on other morphological and molecular criteria, such as elongated shape and apical morphology in early stage 11. At that stage, the floor precursors can be recognized by their distinctive trapezoidal apices (Fig. 4B inset, magenta), the adjacent roof cell apices are more isodiametric (Fig. 4B inset, green), and both can be distinguished from the unconstricted apices of the more posterior main-body follicle cells (Fig. 4B inset, light gray).

We do not consider molecular markers such as Broad or *rho-lacZ*, which could be turned on and off by different cells during morphogenesis, to be lineage tracers. Although it is not currently possible to specifically monitor *rho-lacZ* or Broad-expressing cells in culture, our studies of fixed egg chambers support the idea that the roof and floor are formed by stable populations of cells (see Results).

Immunofluorescence and staging

Ovaries were fixed and stained as described previously (Jackson and Berg, 1999), except that EDTA was omitted from all solutions to preserve E-cadherin staining and the final concentration of glycerol in the mounting medium was 80%.

The following antisera were used: rat monoclonal anti-*D*E-cadherin 'DCAD2' (1:50; Oda et al., 1994), mouse monoclonal anti-Broad core antibody (1:1000, Emery et al., 1994), and rabbit anti-β-galactosidase (1:3000, Cappel). Primary antibodies were detected using standard dilutions (1:100–1:500) of fluorescently labeled Alexa Fluor secondary antibodies from Molecular Probes. Complete details of these protocols are available upon request.

We staged egg chambers by DIC microscopy based on criteria described by Spradling (1993), followed by confocal analysis of morphogenetic landmarks. This procedure worked well for all stages, although the transitions between late stage 11 and early stage 12 or late stage 12 and early stage 13 egg chambers are continua that cannot be precisely pinpointed. Because *bwk* egg chambers are often dumpless, we staged these samples by confocal analysis of morphogenetic landmarks coupled with DIC analysis of chorion deposition. The dorsal appendage chorion first becomes evident at the very end of stage 11 and is reinforced throughout stage 12.

Culture

Stage 10–14 egg chambers were cultured using methods modified from Petri et al. (1979; Berg and Kiehart, unpublished; see http://berglab.gs.washington.edu/culture/). Briefly, young females were placed in vials with yeast paste and males for 1–2 days. Aluminum culture chambers were assembled with a gas-permeable membrane on the condenser side of the specimen (Kiehart et al., 1994). Using a device to ensure a wrinkle-free surface, we mounted a circular piece of Teflon membrane (Standard Kit Model 5793, Yellow Springs Instrument Co., Yellow Springs, OH) over the hole in the chamber. We secured the membrane with a rubber O-ring (1/2″ ID × 5/8″ OD, ORB-014, -BUNA-N, Small Parts, Inc., Miami Lakes, FL). A thin (approximately 150 μm) uniform smear of high-vacuum grease (Dow Corning, # 976V-5.3 oz) was applied in a ring around the outer edge of the Teflon membrane, serving both as a seal and a spacer.

Next, ovaries were dissected in sterile room-temperature 1 × Schneider's *Drosophila* medium (BRL-Gibco, # 350-1720AJ) and carefully separated into individual egg chambers, removing as much muscle sheath as possible. Large stage 10 egg chambers were selected and transferred by Drummond microcapillary pipette (25λ, Drummond Scientific Co., Broomall, PA) into fresh medium, rinsed, then transferred onto the center of a clean cover slip (22 mm^2, #1 or 1.5, Corning, Big Flats, NY). The observation chamber was then inverted so that the grease faced the cover slip and pressed lightly onto the cover slip to pick it up. After righting the chamber, the cover slip was pressed lightly, if necessary, to achieve flatness and a good seal. Samples mounted in this way were imaged through the cover slip on upright and inverted microscopes (see below). After mounting, imaging was initiated as soon as possible, although development sometimes did not resume for approximately 1 h.

An earlier study reported no developmental delay when egg chambers were cultured in the absence of imaging (Petri et al., 1979). We observed variable and longer developmental times and occasional photobleaching when extensive imaging in the *z*-dimension, sometimes necessary for our morphogenetic analysis, was used. Robb's (1969) R-14 complete culture medium was also tested but did not produce significantly different results.

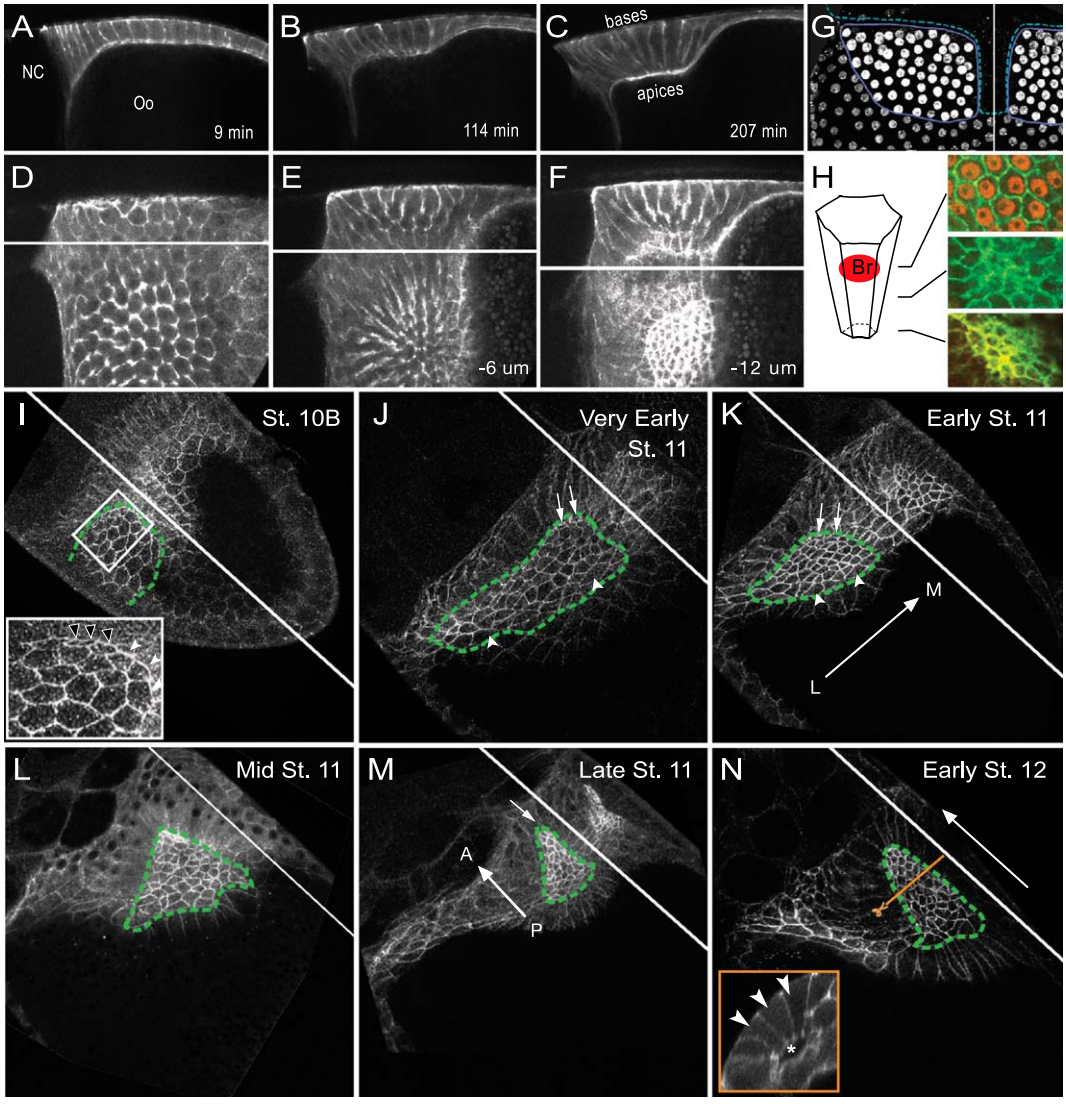

Fig. 2. Hallmarks of tube roof formation in wild-type egg chambers: roof-forming cells elongate, constrict their apices, and express high levels of Broad. (A–F) cultured egg chambers expressing GFP-Moesin throughout the follicular epithelium. (A–C) A lateral section of a stage 10B–11 egg chamber; anterior is to the left. Follicle cells (FCs) in the dorsal anterior of the columnar epithelium elongate over time. Times shown represent minutes in culture; Oo = Oocyte; NC = nurse cell. The full time-lapse sequence, featuring larger views of this and subsequent events, is displayed in Movie 1 Part 1. (D–F) Dorsolateral view of an early stage 11 egg chamber; anterior is to the left and a white line marks the dorsal midline. Descending confocal sections through the follicular epithelium from more basal (D) to apical (F) regions reveal the decreasing diameter of the apically constricted roof cells. The complete *z*-series of the egg chamber featured in D–F can be viewed in Movie 1 Part 2. (G) Dorsal view of a stage 11 egg chamber. Anterior is up, dorsal midline is marked by a white line. Roof cells (inside solid blue line) express high levels of Broad ("high-Broad cells") while floor and centripetal FCs (inside dashed blue line) do not express Broad; main body FCs (outside blue lines) express intermediate levels. (H) Schematic of apically constricted cell. (H, insets) Roof cells in stage 11 w^{1118} egg chamber double stained to show Broad-positive nuclei (red) and cell cortices (ECAD, green). Descending confocal sections reveal the apical constriction of the high-Broad roof cells. (I–N) Optical projections of wild-type egg chambers fixed and stained to detect ECAD to illustrate the changing configuration of the roof cell apices (inside green lines). All samples in I–N are at the same magnification. Anterior is at the upper left. A white line marks the dorsal midline; the lateral-to-medial direction is indicated by a long arrow in K. (I) Cells at the anterior border of the roof cell population initiate apical constriction (black arrowheads, inset), followed at a slight delay by cells at the medial border (white arrowheads, inset). Laterally positioned cells in the dorsal appendage primordium are not featured in this projection. Next, apical constriction progresses to more posterior and lateral cells in the primordium (J) until all the roof cells are constricted apically (K). A gradient of apical cell size exists within the population: the least constricted cells reside at the posterior (arrowheads, J, K) and the most constricted cells arise at the dorsal anterior corner (arrows, J, K) and will eventually lie at the tip of the forming tube (culture data, not shown). By the end of stage 11, the wide almond-shaped array of constricted roof cell apices (K) transforms into a narrow, anterior-pointing triangle (L, M). This transformation contributes to the proper anterior orientation of the future dorsal appendages. (N) The triangular array of roof cell apices lengthens during anterior extension in stage 12. Orange line indicates the approximate position at which the cross section shown in the inset was made. (N, inset) Software-assisted reslice shows cross section of dorsal-appendage-forming cells from a similarly staged egg chamber expressing GFP-Moesin. This image reveals the tube lumen (asterisk) and confirms the apical constriction of the roof-forming cells (arrowheads).

Microscopy and image processing

Cultured ovaries were imaged with a ×40 Zeiss PlanApo 1.2 NA water immersion objective or a ×60 Nikon PlanApo 1.4 NA Oil objective on a BioRad MRC600 microscope and a ×40 Plan NeoFluar 1.3 NA Oil objective on a Zeiss LSM510 microscope. Fixed ovaries were imaged with a UV ×40 PlanApo 1.25 NA Oil objective on a Leica TCS/SP/MP microscope.

Images of cultured egg chambers were analyzed using Amira 2.0 (TGS, http://www.tgs.com/), the public-domain NIH Image software (developed at the U.S. National Institutes of Health and available at http://rsb.info.nih.gov/nih-image/), and 4-D Turnaround (http://www.loci.wisc.edu/4d/). Images of fixed triple-labeled egg chambers were analyzed in Image J (http://rsb.info.nih.gov/ij/). Measurements of cell area and length were performed in Object Image, which permits tracing over 3D image stacks (http://simon.bio.uva.nl/object-image.html). To evaluate differences in *rho-lacZ* cell length between wild-type and *bwk* egg chambers, we employed the *t* test for two population means with unknown and possibly unequal variances (Schiff and D'Agostino, 1996). Figures were assembled in Adobe Photoshop 7 and Illustrator 10, and movies made in Adobe Premiere 6.5.

Projections

For confocal *z*-series of fixed egg chambers, optical sections were collected 0.5–1 μm apart in the *z*-dimension. Because of the constraints of presenting 3D data on the two-dimensional page, most of the data are presented as projections generated in Image J. It is important to emphasize that

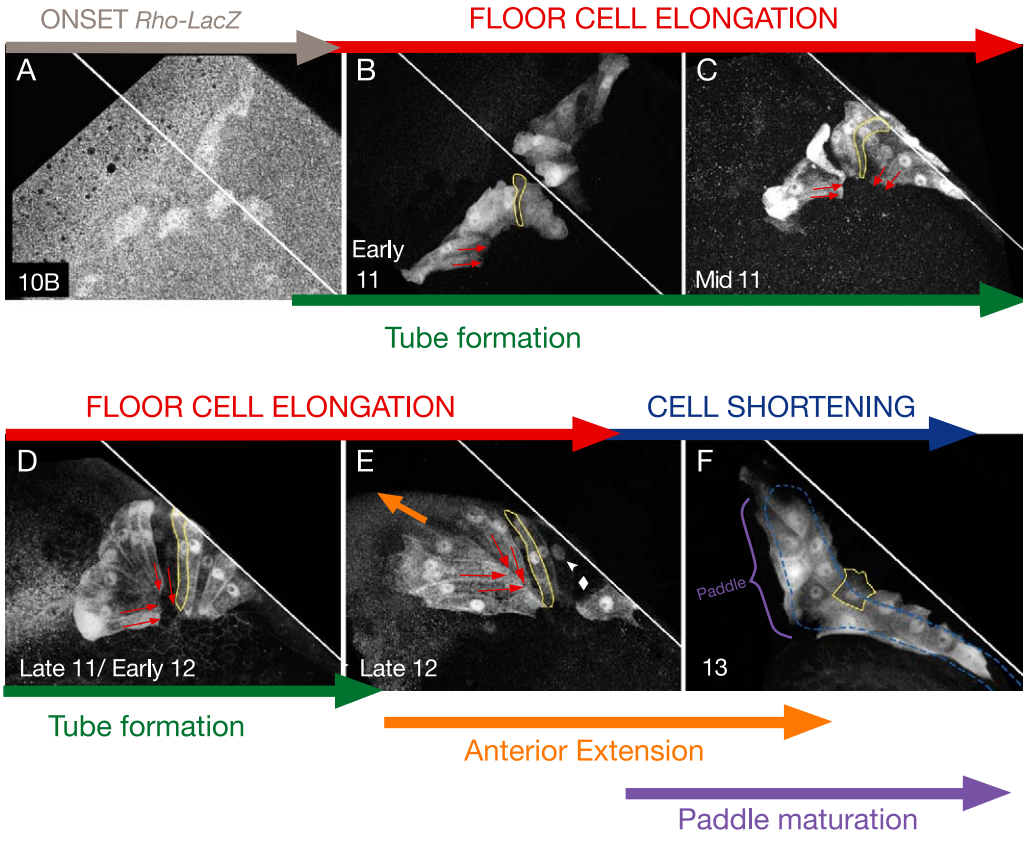

Fig. 3. Three phases of cell-shape change by *rho-lacZ* cells produce the floor of the dorsal appendage. All panels show fixed *rho-lacZ*-expressing egg chambers with anterior at the upper left corner and a white line indicating the dorsal midline. Multiple optical sections are projected for each panel. (A) Dorsal view. In stage 10B, during the first phase of apical-basal elongation that distinguishes all dorsal-appendage-forming cells, the expression of *rho-lacZ* initiates at a low level in floor cell precursors. To detect this low level of expression, a higher gain setting must be used and higher background results. (B) Dorsal view, displaying both dorsal appendage primordia. In each primordium, the *rho-lacZ* cell stripe consists of two rows, one anterior and one medial (parallel to white midline). By early stage 11, the *rho-lacZ* cells in the anterior row begin the floor-specific late phase of elongation (direction of elongation indicated by red arrows). Medial *rho-lacZ* cells initiate elongation shortly thereafter. A representative cell is outlined in yellow at each time point. (C–F) Lateral views, displaying a single dorsal appendage primordium. (C–E) The floor precursors continue their dramatic elongation (red arrows) until, during stage 12, the apices of cells in the anterior row meet the apices of medial row cells. (E) When cells from these two rows meet, they form a continuous floor under the roof cells. In late stage 12, the floor-forming *rho-lacZ* cells form a 'candy cane'-shaped array and, like the roof cells, begin to move towards the anterior (direction of movement indicated by orange arrow). *rho-lacZ* is expressed at variable levels in the floor cells; randomly positioned floor cells display only nuclear expression (e.g., arrowhead in E), while others lack the marker entirely (diamond in E) but are flanked by marked cells. (F) In stage 13, the *rho-lacZ* cells reverse their earlier elongation and shorten. This process helps to create the shape of the mature appendage, which has a narrow stalk and a wide paddle (outlined in blue; the base of the dorsal appendage is outside the field of view).

projections show information that exists in several planes. For this reason, merged images generated from two projections must be interpreted with care; colocalization can only be assigned based on evaluation of single optical sections. Some of the original *z*-series are available as movies in Supplementary Materials; *z*-series not featured there are available upon request.

Reslices

The insets in Figs. 2N and 4D and the images in Movie 4 Part 1 feature reslices of *z*-series data generated in NIH Image, Image J, and Amira 2.0, respectively. Software reslices display information orthogonal to the original collection plane. We noted that single confocal sections occasionally display round cell sections that might be interpreted as comprising local double layering of the roof-forming epithelium, a prediction stemming from the King model. We performed reslice analyses of confocal *z*-series and demonstrated that such images merely transect the epithelium at an angle (see Movie 4). Contrary to the King model, the roof of the tube is a simple monolayer in which every cell spans the entire distance from the basal lamina to the nascent lumen. The floor, too, consists of a monolayer (Fig. 3).

Results

We employed time-lapse confocal imaging of live egg chambers coupled with analyses of fixed, stained tissues to define the morphogenetic events that produce the dorsal appendages. The appendages develop from two primordia that originate near the anterior of the columnar follicular epithelium, flanking the dorsal midline (Fig. 1A). The morphogenetic transformations exhibited by cells in these two primordia, which will generate the left and right dorsal appendages, are symmetrical and mirror each other across the dorsal midline. For simplicity, we will describe the morphogenesis of a single primordium.

We observe three main phases of dorsal appendage morphogenesis. Phase 1: tube formation. In stages 10B, 11, and early 12, the single-layered epithelium transforms into a tube oriented along the A-P axis. Phase 2: anterior extension. From midstage 12 through 13, the tube extends anteriorly over the nurse chamber. Phase 3: paddle maturation. In stages 13 and 14, cells in the distal (anterior) region of the tube remodel and secrete the flattened "paddle." Chorion secretion into the tube lumens begins in very late stage 11; the majority occurs during stages 12–14.

Phase 1: tube formation

Roof forms by apical constriction

Morphogenesis begins at stage 10B when cells in the dorsal anterior region of the follicular epithelium elongate such that their apical–basal height increases, forming a thickened region of the epithelium called a placode (Fristrom, 1988; King and Koch, 1963). To visualize this elongation and subsequent events directly, we employed time-lapse confocal microscopy of cultured egg chambers expressing UAS-GFP-Moesin in all the follicle cells under control of the CY2-GAL4 driver (Bloor and Kiehart, 2001; Dutta et al., 2002; Queenan et al., 1997). GFP-Moesin binds filamentous actin in the cell cortex without deleterious effects and is an excellent reagent for visualizing morphogenesis in living tissue (Dutta et al., 2002; Edwards et al., 1997; Kiehart et al., 2000). The thickening of the dorsal anterior region during stage 10B contrasts markedly with the coincident thinning and spreading of the remainder of the columnar follicular epithelium, which occurs to accommodate the increasing oocyte volume during transfer of cytoplasm (dumping) from the nurse cells. This early elongation and subsequent morphogenetic events can be seen in Movie 1 Part 1.

The dorsal appendage primordium is made up of two cell types whose behavior, morphology, and gene expression patterns diverge after the early elongation of placode formation (Figs. 1A–F vs. A′–F′). These two populations form the roof and the floor of the cellular tube encircling the dorsal appendages and can be distinguished by early stage 11. By the end of the tube formation phase, roof cells cover the dorsal surface of the forming appendage, while floor cells line the ventral surface. To explain the subsequent steps of dorsal appendage formation, we will first give a morphological and molecular account of the roof cells, followed by a similar analysis of the floor cells.

Immediately after elongating, the roof precursor cells within each dorsal appendage primordium change from columnar to wedge-shaped by constricting their apices (a), which in this epithelium are oriented toward the interior, adjacent to the oocyte (Figs. 1H and H′). The adherens junctions encircle each cell just basal to the apical cell surface. These junctions are labeled intensely with both GFP-Moesin and rhodamine–phalloidin, indicating a high concentration of filamentous actin (Figs. 2C and F). We take advantage of these brightly stained adherens junctions to determine the shape of the apical portions of dorsal-appendage-forming cells. Apical morphology distinguishes dorsal appendage cells from their neighbors more clearly than basal surface views and even differentiates floor from roof cells as early as stage 11 (see Materials and methods). Apical constriction is best appreciated by examining confocal sections that descend from the basal surface of the epithelium. Such a *z*-series, shown in Movie 1 Part 2, reveals the decreasing roof cell diameter as one approaches the apical surface (See Movie 1 Part 2 and stills excerpted in Figs. 2D–F; apical $\text{area}_{\text{early11}} = 56\ \mu\text{m}^2$, SD = 25, $n = 42$; basal $\text{area}_{\text{early11}} = 164\ \mu\text{m}^2$, SD = 22, $n = 22$).

We also visualize adherens junctions by detecting the key constituent protein E-cadherin (ECAD) by immunocytochemistry. By imaging cell apices in fixed tissue with this reagent, we find that apical constriction is patterned both in space and time. Apical constriction does not happen syn-

chronously in all roof-forming cells but rather occurs progressively in a defined manner. In late stage 10B, cells at the anterior and medial edges of the population initiate apical constriction (black and white arrowheads, respectively, in Fig. 2I inset); and in early stage 11, cells located posterior and lateral of them follow suit (Figs. 2J and K). Even when apical constriction is well underway, cells at the posterior of the population remain less constricted (arrowheads in Figs. 2J and K).

After the roof population constricts apically, it narrows mediolaterally and lengthens anterior–posteriorly. Whereas in early stage 11, the roof cell population is elongated mediolaterally (= left-right; Fig. 1B); by the end of stage 11, it is more circular (Fig. 1C). This reconfiguration can be detected at the level of the roof cell apices where an initially almond-shaped array (Fig. 2K) transforms into a short, anteriorly directed triangle (Figs. 2L and M). During this reorganization, the roof cells constrict their apices further; by late stage 11, they are twofold smaller than in early stage 11 (apical $area_{late11}$ = 25 μm^2, SD = 7, n = 32; Figs. 2M vs. K). This continued constriction reduces the overall medial–lateral extent of the population. Roof-forming cells may also intercalate during this process (see Discussion). The observed change in shape of the roof cell array is important for the proper narrowing of the nascent tube and for proper anterior–posterior orientation during its subsequent elongation.

Roof cells express high levels of Broad

To relate these morphological events to known molecular markers for dorsal-appendage-forming fate, we double-stained egg chambers with rhodamine–phalloidin, which binds filamentous actin, and with antibodies against the conserved core domain of the Broad protein (Emery et al., 1994). *broad* (*br*) encodes a zinc-finger transcription factor required for dorsal appendage formation (Deng and Bownes, 1997; Tzolovsky et al., 1999). During late oogenesis, BR responds to both the EGFR and TGF-β pathways and provides a read-out for the intersection of these two signaling processes during patterning (Deng and Bownes, 1997). Hence, from stage 10B on, BR is often used as a fate marker for the dorsal-appendage-forming follicle cells. We find, however, that only a specific subset of the dorsal-appendage-forming cells expresses high levels of Broad during morphogenesis—namely, the roof-forming cells. The roof precursors (hereafter called 'high-Broad cells,' Fig. 2G, outlined by solid line; Fig. 2H) express elevated levels of BR before apical constriction and throughout the morphogenetic process (for example, Figs. 1A–F and A′–F′ and Movie 2). In contrast, main-body follicle cells express lower levels of BR (Fig. 2G, not outlined). Cells on the dorsal midline and in several rows at the dorsal anterior of the columnar epithelium, which eventually overlie the operculum, express negligible levels of BR (Fig. 2G, outlined by dashed line; Tzolovsky et al., 1999). The number of high-Broad cells is constant throughout dorsal appendage formation (52.4 ± 6, French et al., 2003; Berg and Ward, unpublished observations).

Although Broad protein is expressed at high levels in the roof-forming cells described thus far, it fails to mark the cells that form the floor portion of the tube. Moreover, reagents that label filamentous actin, both in live and fixed tissue, resolve these (ventral) floor cells poorly. This property may result from several attributes of these cells: a more diffuse distribution of filamentous actin, a deeper location within the tissue, or an extremely thin morphology.

Visualizing floor cells with rho-lacZR1.1

Since markers that highlight the actin cytoskeleton failed to label clearly those cells that create the floor of the tube, we looked for other ways to visualize floor formation. We identified a marker that labels the floor-forming cells: *rhomboid-lacZR1.1 (rho-lacZ)*. In this construct, a 2.2-kb fragment of the *rhomboid-1* promoter drives expression of a *lacZ* reporter (Ip et al., 1992). The *rhomboid-1* gene is expressed in a subset of follicle cells where it is required for the amplification and refinement of EGFR signaling activity that produces two groups of dorsal-appendage-fated cells (Bang and Kintner, 2000; Lee et al., 2001; Nilson and Schüpbach, 1999; Peri and Roth, 2000; Ruohola-Baker et al., 1993; Urban et al., 2001, 2002; Wasserman and Freeman, 1998). The *rhomboid-lacZR1.1* reporter differs from the endogenous *rhomboid-1* gene in several useful respects. First, the spatial extent of expression is more restricted. *rhomboid-1* mRNA is expressed initially in a 'saddle'-shaped domain encompassing all the dorsal-appendage-forming cells (Ruohola-Baker et al., 1993). We find that the *rho-lacZ* reporter, however, is expressed exclusively in floor-forming cells (see below). Second, the time window of reporter expression is shorter and more specific to dorsal appendage formation. While *rhomboid-1* is expressed before morphogenesis begins, starting at stage 9 of oogenesis (Ruohola-Baker et al., 1993), *rho-lacZ* turns on in stage 10B (Sapir et al., 1998, and this work) and remains on through stage 14 (Fig. 3 and data not shown). Furthermore, although the Rhomboid protein is localized to apical membranes (Ruohola-Baker et al., 1993), β-Galactosidase driven by the *rho-lacZ* reporter fills the cytoplasm, facilitating observation of the elaborate shape changes that floor-forming cells undergo during morphogenesis.

Although we have not performed a lineage analysis of floor precursors, the floor of the tube appears to be constructed by a stable population of *rho-lacZ*-positive cells. After a phase in late stage 10B and early stage 11 during which *rho-lacZ* expression is still initiating (Fig. 3A), the number of *rho-lacZ* cells per dorsal appendage primordium stabilizes at 10–15 cells ($mean_{wt}$ = 11.3 cells/appendage, SD = 1.8, n = 418 cells from 37 appendages). At least some of the observed range in *rho-lacZ* cell number derives from the reporter's variable and patchy expression (see Materials and methods). The shape changes and movements exhibited by the *rho-lacZ* cells form a tight sequence that proceeds incrementally through both space and time (Fig. 1A′–F′). We describe these behaviors in more detail below.

rho-lacZ cells border high-Broad population at the beginning of morphogenesis

rho-lacZ turns on in stages 10B and early 11 in two hinge ('Γ')-shaped domains, one on either side of the dorsal midline (Figs. 3A, B and 4C; Sapir et al., 1998). To simplify the discussion, we describe the behaviors of cells in a single primordium; mirror-image processes occur on either side of the dorsal midline. Each 'Γ' of *rho-lacZ* cells is composed of a stripe of cells, one cell wide, which bends through 90° at the dorsal anterior corner. Within the stripe, a medial row of approximately 5–7 cells runs parallel to the dorsal midline (i.e., from posterior to anterior, Fig. 1B′; outlined in purple in Fig. 4C), and an anterior row of roughly 6–8 cells is oriented perpendicular to the midline (i.e., from medial to lateral = dorsal to ventral; Fig. 1B‴; outlined in red in Fig. 4C).

Before morphogenesis begins, all follicle cells express BR (Deng and Bownes, 1997; Tzolovsky et al., 1999) but from stage 10B until the end of oogenesis, the *rho-lacZ* follicle cells consistently lack BR staining (e.g., Fig. 4D inset). Throughout dorsal appendage formation, the *rho-lacZ* floor precursors remain physically adjacent to the high-Broad roof precursors (Fig. 1A–F). During the earliest events of dorsal appendage formation, for example, in stages 10B and 11, *rho-lacZ* floor cells directly abut the dorsal and anterior margins of the high-Broad (roof) population. This 3D configuration is best appreciated by examining the *z*-series shown in Movie 2 (single section excerpted in Fig. 4D).

Directed cell elongation forms floor

How do the *rho-lacZ* cells come to lie underneath the roof cells? Initially, the anterior row of *rho-lacZ* cells resides posterior to several rows of centripetal cells (Fig. 1G). As the centripetal cells migrate down between the oocyte and the nurse cells (Figs. 1H and 4D inset), the *rho-lacZ* cells are pulled forward until the anterior row of *rho-lacZ* cells reaches the anterior margin of the columnar epithelium (Fig. 1I). These movements cause the anterior row of *rho-lacZ* cells to tilt relative to the surface of the egg chamber such that their apices lie posterior of their basal surfaces (Fig. 4D inset). This process positions the cells to begin their posterior-ward elongation.

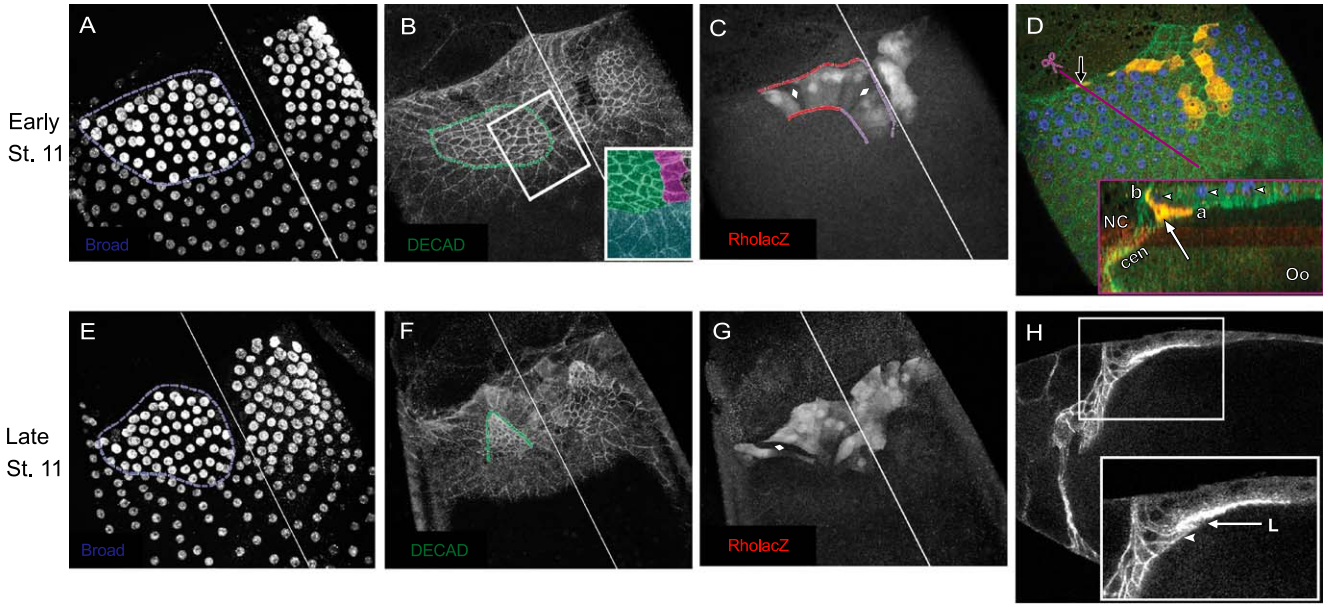

Fig. 4. In wild-type oogenesis, stage 11 encompasses dynamic changes in both roof and floor precursors in a short period of time. All panels show fixed egg chambers; the dorsal midline is indicated by a white line. Anterior is at the left in H and at the upper left in all other panels. D and H show single optical sections; other panels are projections of multiple optical sections. (A–D) Early stage 11 egg chamber. (E–G) Late stage 11 egg chamber. (A, E) The roof-forming cells (outlined in blue) express high levels of BR. (B, F) ECAD staining reveals that the apices of these roof-forming cells (outlined in green) compose an almond-shaped array in early stage 11, while by late stage 11 they adopt triangular arrays of more tightly constricted apices. (B, inset) Roof, floor, and main body FCs can be identified based on distinct apical morphology in early stage 11: floor cells have trapezoidal apices (magenta), while roof cell apices are smaller and more isodiametric (green) and the main body follicle cells are unconstricted (light gray). (C) In each primordium, floor cells are arranged in a "Γ"-shaped stripe consisting of an anterior row of 6–8 cells (bases = dashed red line, apices = solid red line) and a medial row of 5–7 cells (bases = dashed purple line, apices = solid purple line). Scattered floor cells (diamonds) do not express the *rho-lacZ* marker. (D) A single section near the basal surface of the epithelium demonstrates that the basal portions of the floor cells (*rho-lacZ*, red) abut the anterior and medial borders of the roof cell population (high Broad, blue). See entire *z*-series in Movie 2. (D, inset) The *z*-series is resliced using Image J software along the magenta line in D to show the shape of the bisected floor cell (black arrow in D). At this early stage 11 time point, the anterior-row floor cells (white arrow) narrow their basal footprint (b), drop their nuclei (arrow) down under the high Broad nuclei (arrowheads), and begin to elongate their apices (a) under the high-Broad roof cells. NC = nurse cell; cen = centripetal cells; Oo = oocyte. (G) Projections of the floor cells reveal increasing elongation as stage 11 proceeds (compare to 4C; see also Figs. 3B–D). (H) A single lateral optical section showing a different late stage 11 egg chamber, stained with antibodies against ECAD. Anterior is to the left. The elongation of the floor cells (arrowhead, inset) under the roof cells creates a small lumen (L) (arrow, inset).

Next, the *rho-lacZ* cells begin a phase of pronounced elongation to form the floor. This floor-specific elongation is subsequent to the elongation that all dorsal-appendage-forming cells undergo in stage 10B. This second phase of elongation ('late elongation') begins in stage 11, while the high-Broad roof cell apices assume a triangular configuration (Figs. 4B and C vs. F and G). Late elongation creates the floor of the tube and involves the coordinated movement of *rho-lacZ* cells from both anterior and medial rows of the 'Γ' hinge, as described below.

In stage 11, the *rho-lacZ* cells in the anterior row of the 'Γ' begin to extend underneath the high-Broad cells (Fig. 1B′, arrow; Fig. 1H; Fig. 3B, arrows). The medial row of *rho-lacZ* cells soon undergoes a similar elongation (Fig. 1C′, arrow; Figs. 1I′and 3C). Cells from the anterior and medial rows of the 'Γ' elongate towards each other until, in mid-stage 12, their apices meet and fuse (Figs. 1B′–D′and 3B–E). Confocal *z*-series demonstrate that the *rho-lacZ* cells from the medial row project their apices deep and posterolaterally while the anterior row of *rho-lacZ* cells project apices deep and posteromedially (Figs. 1C′and 3C). During elongation, the *rho-lacZ* cells constrict their basal surfaces, drop their nuclei below the high-Broad cells, and extend their apices, stretching the cytoplasm thin in the process (Figs. 1H, I, and 4D inset). In late stage 11 and early stage 12 egg chambers, the floor cells form a 'fan' (Figs. 1C′and 3D). By late stage 12, the floor cells compose a 'candy cane'-shaped array, which is two cells wide at the anterior and one cell wide at the posterior (Figs. 1D′and 3E). This layer of elongated *rho-lacZ* cells forms the floor underneath the high-Broad roof cells and in so doing completes the basic topography of the tube (Fig. 1J and J′).

Phase 2: anterior extension

Unlike the *Drosophila* malpighian tubules and the mammalian kidney, which elongate by cell division (Ainsworth et al., 2000; Schöck and Perrimon, 2002), the dorsal appendages lengthen exclusively by cell shape-change and movement. After the roof- and floor-forming cells form a tube, they move anteriorly over the nurse chamber. This movement, which takes place in stages 12 and 13, lengthens the tube inside which chorion will be secreted; thus, anterior extension creates dorsal appendages of normal dimensions. We examined this anterior-extension process in cultured egg chambers (Figs. 5A–C). Underneath the constricted apices of the advancing roof cells, the lumen grows from posterior to anterior (arrowheads mark anterior limit of lumen in Figs. 5E and F). Beneath the lumen, the floor cells also move anteriorly. This anterior movement of the *rho-lacZ* cells stretches the formerly 'fan'-shaped array into a 'candy cane' shape in late stage 12 (Figs. 1C′, D′, 3D, and E).

As the floor-forming *rho-lacZ* cells move anteriorly, they contact two distinct substrates. Until late stage 12, the *rho-lacZ* cells rest entirely on top of the centripetal cells (Figs. 1H and I and data not shown). Only in late stage 12, when anterior extension is underway, do the *rho-lacZ* cells begin to move anterior of the centripetal cells over the nurse cells. Even at this stage, however, the posterior-most *rho-lacZ* cells, those formerly at the posterior end of the medial stripe, rest on top of centripetal cells (Fig. 1J and data not shown). The *rho-lacZ* cells that move forward over the nurse cells do not contact the nurse cells directly but instead move on an intervening layer of extremely thin stretch cells (not shown in Fig. 1; Tran and Berg, 2003; Ward and Berg, unpublished results).

Phase 3: paddle maturation

During paddle maturation, both roof and floor cells again change shape. In stage 13, roof cells increase their apical surface area, reversing their earlier apical constriction (blue cell footprints in Figs. 1E vs. D). At the same time, the *rho-lacZ* cells change shape on the inner surface of the paddle. This process involves a shortening along the apical–basal axis, a reversal of their earlier elongation (Figs. 1E′vs. D′and 3F vs. E). Together, these shape changes in the roof and floor create the mature shape of the paddle, which is wider and flatter than the cylindrical stalk. The increased width of the paddle relative to the stalk is correlated with three asymmetries: (1) The roof cell array is 4–5 cells wide over the paddle and only 3–4 cells wide over the stalk (Figs. 1E and 8A). (2) Roof cells over the paddle expand their apices more than roof cells over the stalk (data not shown). (3) The floor cell array under the paddle is two cells wide, while under the stalk it tapers and then becomes one cell wide (Figs. 1E′and 3F).

During stages 12 and 13, as the nurse cell volume decreases, the dorsal appendage primordia rotate. The *rho-lacZ* cells maintain their position under the high-Broad cells, although the whole dorsal-appendage-forming unit rotates from the top of the egg chamber down around the side of the egg chamber. Thus, the roof cells, which were formerly dorsal, become lateral and the *rho-lacZ* cells, formerly ventral, become medial (Figs. 1J′ and K′). Nevertheless, the roof cells remain on the outer surface of the appendage, while the floor cells continue to line the inner surface. From stage 13 on, the *rho-lacZ* cells line the inner surface of the paddle and the anterior portion of the stalk (Figs. 1F′, L, L′, and 3F). Posteriorly, these *rho-lacZ* cells separate the dorsal appendages from the nurse and stretch cells; at the anterior, they separate the two paddles.

Morphogenesis begins normally in bullwinkle mutants

The molecular and morphological features of wild-type floor and roof-forming cells provide a basis for interpreting defects in mutants with abnormal dorsal appendages. The vast majority of such mutants affect dorsal appendage formation by disrupting the patterning of the appendage primordia. To focus on the process of morphogenesis specifically, we have analyzed the *bullwinkle (bwk)* mutant, which accomplishes the initial patterning normally but displays moose-antler-shaped dorsal appendages (Rittenhouse

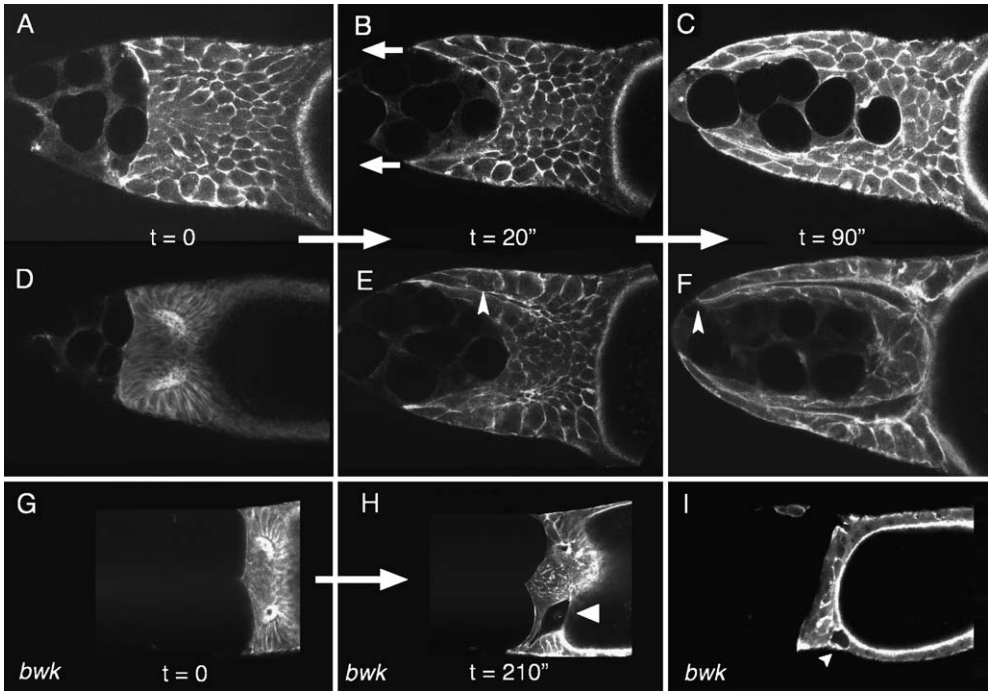

Fig. 5. Frames from time-lapse movies of cultured wild-type (A–F) and *bullwinkle* (G–I) egg chambers expressing GFP-Moesin. All panels display dorsal optical sections, except panel I, which shows a lateral section. Anterior is to the left. (A, D, G) Stage 11 egg chambers. (B, E, H) Stage 12 egg chambers. (C, F, I) Stage 13 egg chambers. (A–C) Sections taken near the basal surface at successive time points reveal movement of the dorsal-appendage-forming cells towards the anterior of the egg chamber (left arrows in B). (D–F) Deeper (more apical) sections at the same time points reveal the progress of the lumen, which is advancing forward inside the tube. White arrowheads in E and F mark the anterior limit of the right lumen. By stage 13, the lumen reaches the front of the tube. Due to a slight tilt in the egg chamber, the lumen can only be followed along its entire length in the upper (right) dorsal appendage in this optical section. (G) Although apical constriction occurs normally in cultured *bwk* egg chambers, anterior extension is abnormal. The dorsal appendage-forming cells commonly do not advance to the anterior of the egg chamber, the two dorsal appendages are often asymmetrical, and the shape of the lumens is frequently aberrant (arrowhead, H). The follicular epithelium did not advance anteriorly at later time points. See Movie 3 for time-lapse movie of egg chamber featured in G and H. (I) A lateral section of a different cultured *bwk* egg chamber, anterior to the left. The follicle cells appear disordered and gaps are present in the Moesin staining, suggesting defects in cell adhesion (arrowhead).

and Berg, 1995). The chorion defects include short and wide stalks, short and wide paddles with irregular edges, and occasional small spurs or prongs (Rittenhouse and Berg, 1995). To understand the *bwk* eggshell phenotype, we investigated the nature of the morphogenetic abnormalities that generate *bullwinkle* dorsal appendages.

We envisioned several potential mechanisms that could generate the short, broad moose-antler-shaped appendages of *bwk* egg chambers. The appendages may remain too wide, for example, if the apices of the roof-forming cells do not constrict. Alternatively, *bwk* appendages may result from the failure of the apically constricted population to reconfigure during stage 11 from a short, wide almond-shaped array to a long, narrow array. Furthermore, aberrant floor cell movements or shapes or abnormal anterior extension could cause the mutant's short, wide appendages. To investigate these possibilities, we employed several complementary approaches. First, we visualized roof-forming cells in fixed *bwk* egg chambers by immunocytochemistry with antibodies recognizing BR and ECAD. Second, we analyzed the contribution of the *rho-lacZ* cells to the *bwk* phenotype. Third, we observed cell shapes and movements in cultured *bwk* egg chambers by expressing GFP-Moesin throughout the follicular epithelium. In both cultured and fixed *bwk* egg chambers, stages 10B and early 11 proceed normally. Normal numbers of roof-forming cells express high levels of BR and constrict apically (data not shown), while *rho-lacZ* turns on correctly in "Γ"-shaped rows consisting of the wild-type numbers of cells ($mean_{bwk}$ = 12.3 cells/appendage, SD = 1.7, n = 221 cells from 18 appendages). Analyses of later stages, however, revealed cell shape and movement defects in both the roof and floor cell populations, suggesting possible mechanisms for *bwk* action.

bullwinkle defects in roof and floor subpopulations

In *bullwinkle* mutants, defects in both roof and floor formation become evident shortly after morphogenesis begins. Although apical constriction occurs normally in roof cells, the roof cell apices usually fail to reorganize from an almond shape into a normal triangular array by late stage 11 (7 of 8 fixed egg chambers). Instead, *bwk* roof cells form a blunt array that, even in stage 12, is abnormally short (Figs. 6F vs. B) and/or wide (Figs. 7F vs. B). Thus, *bwk* mutations do not affect individual roof cell shape per se but rather impair the coordination and movement of the roof cell population.

Floor formation is also impaired in *bwk* egg chambers. Although *bwk* floor cells begin to elongate normally,

extending beneath the nascent roof in late stage 11, they display defects in several subsequent stages. During tube formation, *bwk* floor cells frequently separate along their basolateral margins (Figs. 6G and K, arrowheads, vs. C) and the most lateral *rho-lacZ* cells of the anterior row often project too far laterally, sticking out of the fan (brackets in

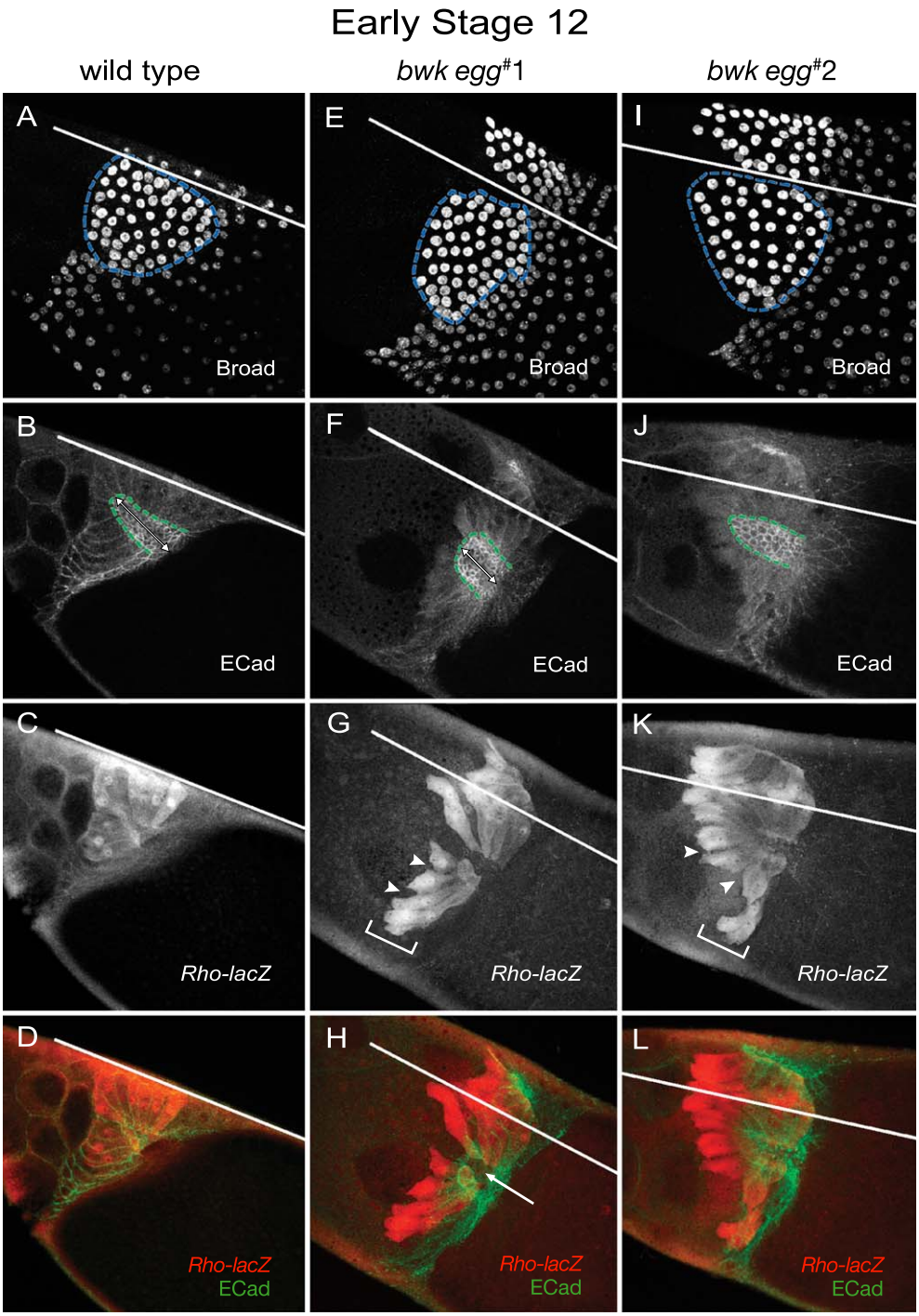

Fig. 6. By early stage 12, *bullwinkle* egg chambers display defects in both roof and floor formation. (A–D) Lateral views of a fixed wild-type egg chamber, anterior at the top left. Projections show nuclei (A, blue outlines) and constricted apices (B, inside green outlines, ECAD) of the high-Broad roof cells. Underneath these roof cells are the elongated cytoplasms of the *rho-lacZ* cells (C) whose apices come together to form a continuous floor surface (see merge in D). (E–H and I–L) Dorsolateral views of two different fixed *bwk* egg chambers. Dorsal midlines indicated by white lines. (B, F) The apically constricted roof cell population often does not narrow mediolaterally and lengthen anteroposteriorly as far as wild type (arrows mark length). (G, H, K, L) *bwk* floor cells often separate along their basal margins (arrowheads), extend too far laterally (brackets in G and K), and display apical gaps that result in an incomplete tube floor (arrow in H, three of five stage 12 egg chambers). (I–L) Even when the *bwk* roof population attains normal length (J), *rho-lacZ* floor cells often extend too far laterally (K, bracket) and exhibit basal discontinuities (arrowheads).

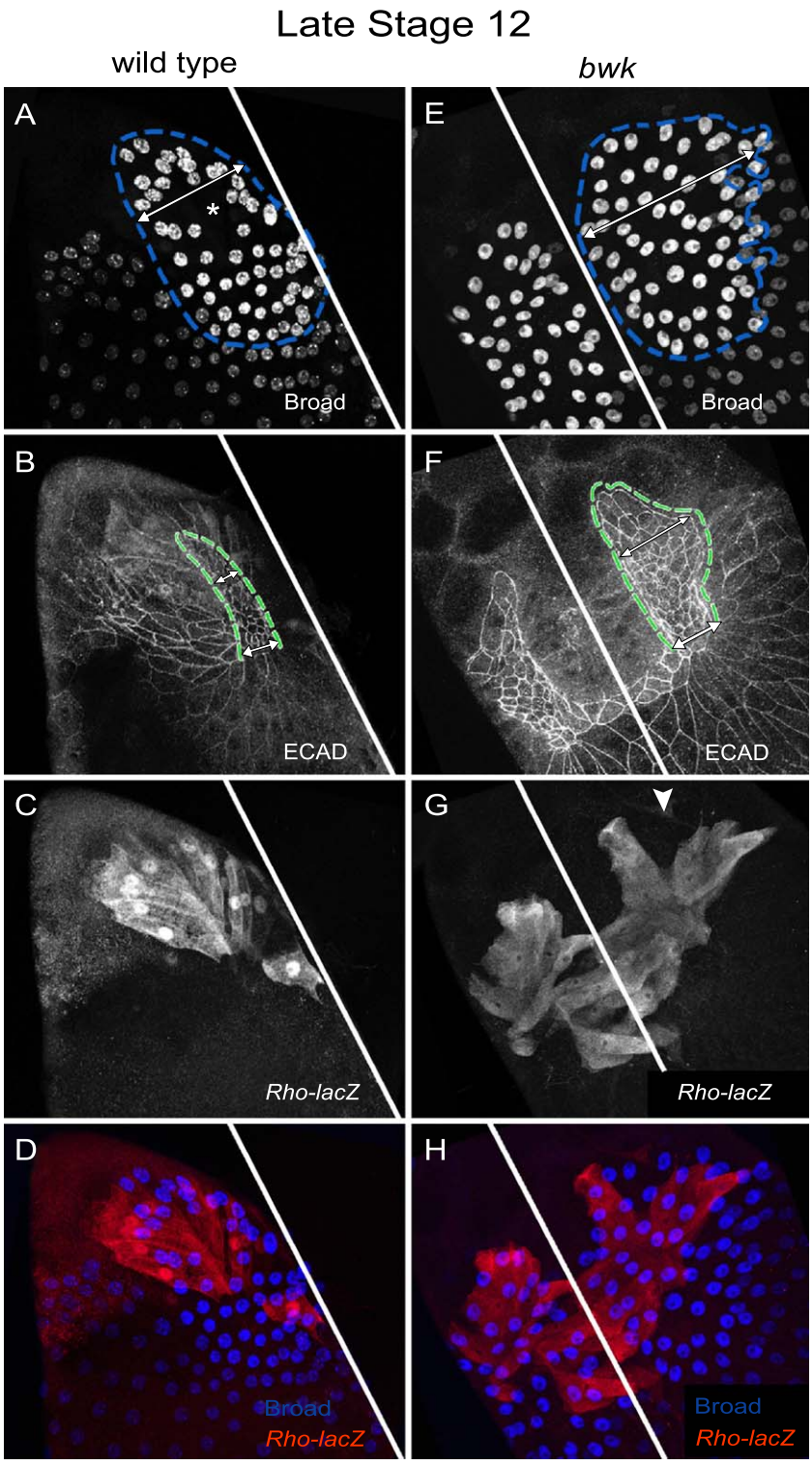

Fig. 7. By late stage 12, *bullwinkle* egg chambers display severe defects in both roof and floor formation. (A–D) Lateral views of a fixed wild-type egg chamber and (E–H) dorsal views of a fixed *bwk* egg chamber, anterior at top of white lines, which indicate dorsal midline. (A, E) Projections show that the high-Broad roof cell population (outlined in blue) is wider mediolaterally in *bwk* than in wild type (arrows). Note: *z*-series in A did not capture all of the high-Broad nuclei in the area marked by the asterisk. (B, F) The roof cell apical array (ECAD, outlined in green) is also abnormally wide (arrows). (C, G) The *bwk* floor cell population displays clefts (arrowhead, G) and disordered abnormally wide arrays at the 'candy cane' stage. (D, H) Merge of the projections in A and C and E and G showing the roof cell nuclei (Broad, blue) over the floor cell cytoplasms (*rho-lacZ*, red).

Figs. 6G and K). Occasionally, the *rho-lacZ* cells fail to meet and fuse properly, resulting in a discontinuous floor (Figs. 6G and H vs. C and D). Since the floor cells remain attached to roof cells along the sides of the tube throughout wild-type morphogenesis and since the roof cell population displays an abnormal configuration, defects in floor formation might be a secondary consequence of defects in roof morphogenesis (or vice versa). Rarely, however, *bwk* egg chambers produce a roof array of normal dimensions (Fig. 6J); these egg chambers still exhibit *rho-lacZ* cell abnormalities (Fig. 6K), suggesting that the *bwk* floor defects are independent of roof cell behavior.

Following this aberrant tube formation, anterior extension often occurs abnormally in both fixed and cultured *bwk* egg chambers. Movie 3 shows how anterior extension begins normally but subsequently stalls before the appendage-forming cells reach the anterior end of the egg chamber (Movie 3, excerpted in Figs. 5G and H). In addition, fixed and cultured *bwk* egg chambers frequently display aberrantly shaped tube lumens that are either bent or expanded (Movie 3 and Fig. 5H, arrowhead). This phenotype may result from a compression of the tissue due to incomplete anterior extension. Alternatively, it may reflect a misregulation of tube diameter (Lubarsky and Krasnow, 2003) or the inability of tube-forming cells to adhere to the chorionic extracellular matrix. Cultured *bwk* egg chambers exhibit other defects consistent with abnormal adhesion, including rounded-up and delaminating follicle cells (arrowhead, Fig. 5I).

During anterior extension, the floor cell population becomes increasingly disorganized, often forking around large clefts (Figs. 7G, arrowhead, and Fig. 8F, arrow). This phenotype may represent a more advanced stage of the basolateral discontinuities we observed in stage 11. The roof cell population can also bifurcate (arrow, Fig. 8E). This bifurcation of the tube correlates with the secretion of prongs and spurs of chorion that project off the main dorsal appendage in the mutant (Figs. 8E–H).

Finally, *bwk* floor cells display defects during paddle maturation. Because *bwk* paddles are wider than those present on wild-type egg shells, we hypothesized that the *rho-lacZ* cells do not shorten properly during paddle formation. To test this prediction, we compared the length of *rho-lacZ* cells in fixed stage 13 wild-type and *bwk* egg chambers. We find that the *bwk rho-lacZ* cells indeed remain 27% more elongated during paddle formation than wild-type cells (wt = 26 μm, SD = 10, $n = 31$ cells; *bwk* = 33 μm, SD = 12, $n = 36$ cells; $P < 0.01$; see Materials and methods.) Thus by late stage 13, the abnormally wide shape of the *bwk* moose-antler appendages (Fig. 8H) is prefigured by the abnormally elongated configuration of the *rho-lacZ* cells (Figs. 8F and G).

Discussion

Dorsal appendage formation is an attractive model because it provides a relatively simple and yet multifaceted example of epithelial morphogenesis. In this discussion, we highlight the important features of wild-type dorsal appendage morphogenesis, contrast our findings with earlier models of dorsal appendage formation, and draw parallels with known morphogenetic events. In addition, we use our analysis of the *bullwinkle* mutant to generate hypotheses about the molecular mechanisms of *bwk* pathway function.

The dorsal-appendage-forming cells undergo shape changes and movements that are tightly controlled in space and time, with subpopulations carrying out distinct behaviors at precise periods. Indeed, our work emphasizes the fact that the dorsal appendage-forming cells are not a single cohort. We distinguish two subpopulations of dorsal appendage-forming cells by molecular and morphological criteria (see Table 1). While previous investigators assumed that dorsal-appendage-forming cells possess a single cell fate, our studies suggest that these subpopulations represent distinct cellular identities. Furthermore, we establish a link between cell fate and the specific events of morphogenesis by examining molecular markers that reflect the cells' patterning histories and placing these markers into the morphogenetic context. Future studies will illuminate how these subpopulations are specified and maintained as separate entities while also coordinating their behaviors to achieve successful morphogenesis.

In addition to defining the roof and floor subdomains, our detailed morphological analyses have clarified certain key aspects of dorsal appendage formation. The preexisting model of dorsal appendage morphogenesis suggested that a subset of the centripetal cells formed the dorsal appendages by leaving the epithelium to move anteriorly (King, 1970; King and Koch, 1963). This model can now be refined in two important respects. First, our analysis clearly shows that the dorsal-appendage-forming cells do not participate in centripetal migration; instead, the dorsal appendage primordia arise immediately posterior to the centripetal cells. Although they remain closely associated with the centripetal cells, resting on top of them until late stage 12, dorsal-appendage-forming cells compose a morphologically distinct population that is likely to act under separate molecular control.

Second, King (1970) suggested that a ring of cells secretes the base of the dorsal appendages and that subsequent cells migrate over the earlier arrivals to secrete the more distal parts of the appendage (reviewed by Spradling, 1993; Waring, 2000). This model requires that cells move over each other, resulting in temporary double-layering of the roof epithelium. Despite our detailed 3D analysis, however, both fixed and cultured egg chambers provide no evidence of cells exiting the follicular epithelium to move mesenchymally over other cells (see Movie 4, and Reslices section in Materials and methods). Instead, dorsal appendage formation involves the movement of cells in cohesive sheets. Thus, our studies demonstrate that the basic mode of movement of dorsal-appendage-forming cells is fundamentally different than previously thought and more closely resembles *Drosophila* salivary

gland, spiracle, and ventral furrow formation, as well as vertebrate gastrulation and neurulation (Costa et al., 1993; Fristrom, 1988; Hogan and Kolodziej, 2002; Hu and Castelli-Gair, 1999).

Stable apical constriction leads to epithelial curvature and coherence

Tube formation during dorsal appendage development in *D. melanogaster* involves apical constriction of the roof-forming cells. As a consequence of apical constriction, formerly columnar epithelial cells assume a wedge or 'bottle' shape. Apical constriction occurs throughout metazoan development, e.g. during amphibian, fruit fly, and sea urchin gastrulation (Costa et al., 1994; Hardin and Keller, 1988; Kimberly and Hardin, 1998), as well as primary neurulation in chordates (Davidson and Keller, 1999; Smith et al., 1994). In some contexts, apical constriction results from passive deformation by external forces (Bard and Ross, 1982; Fristrom, 1988). Apical constriction of the roof precursors during dorsal appendage formation, however, is likely to be an active cell-shape change. This process occurs in a select subset of columnar follicle cells, precedes the dramatic cell-shape changes of the floor precursors, and contrasts with the uniform flattening that occurs in main-body follicle cells at this time. Furthermore, *Ras* null follicle cells do not constrict apically, even when surrounded by constricting wild-type cells (James et al., 2002). Finally, the accumulation of apical actin in roof cells is consistent with active contraction by an actomyosin purse-string mechanism, which has been hypothesized to cause apical constriction in other contexts, including gastrulation (Leptin et al., 1992; Young et al., 1991).

Unlike amphibian, sea urchin, and fruit fly gastrulation, during which apically constricted 'bottle cells' form only transiently (Hardin and Keller, 1988; Kimberly and Hardin, 1998; Leptin, 1999; Shih and Keller, 1992), dorsal appendage roof cells remain constricted for the majority of morphogenesis. Whereas in many other contexts, apical constriction precedes an epithelial-to-mesenchymal transition, the roof cells never exit the epithelium in which they arise. In both of these respects, dorsal appendage formation more closely resembles vertebrate neural tube and *Drosophila* salivary gland morphogenesis (Colas and Schoenwolf, 2001; Myat and Andrew, 2000; Schoenwolf and Smith, 2000). To understand why the roof cells maintain constricted apices throughout the bulk of dorsal appendage formation, it is helpful to consider the possible functions of apical constriction.

Apical constriction likely plays at least two roles in dorsal appendage morphogenesis. First, apical constriction probably helps to shape the chorionic appendage, which has a cylindrical stalk posteriorly and a flat paddle anteriorly. The apical constriction of the roof-forming cells may physically flex the epithelium, as in amphibian neurulation (Davidson and Keller, 1999). Since the tube of dorsal-appendage-forming cells acts as a mold into which the chorion proteins are secreted, the constriction-induced curving of the roof epithelium translates into the curved shape of the chorionic stalk. If apical constriction creates curvature in the follicular epithelium and the resulting chorion, one would expect the roof cells to unconstrict their apices when forming flat chorionic structures. This apical expansion is indeed observed in stage 13 while the follicle cells are forming the paddle. Second, apical constriction may cause the dorsal appendage-forming cells to adhere more tightly to one another by shortening and concentrating the apically located adherens junctions (Fristrom, 1988). Increased adhesion between the apically constricted roof-forming cells may facilitate morphogenesis by fortifying the epithelium to withstand the mechanical stresses experienced by this morphogenetically active tissue (Tepass et al., 1996).

Change in roof array suggests intercalation

The roof cells, while maintaining constricted apices, undergo a dramatic change in configuration (Figs. 1A–F and 2I–N). The narrowing of the roof population from a wide almond (Figs. 1B and 2J) to a long oval (Figs. 1D and 2N) contributes to the lengthening of the tube and of the dorsal appendage within. Our analysis of the *bwk* mutant demonstrates that if the apically constricted roof cells fail to adopt a forward-pointing triangle configuration and instead remain in the medial-laterally elongated almond, the resulting chorionic appendages will be abnormally wide.

What mechanisms might explain the observed narrowing and lengthening of the roof cell array? Our data suggest that at least three cellular mechanisms may contribute: (1) the continued constriction observed throughout stage 11, in which already apically constricted cells reduce their apical diameters twofold more, contributes to the transition by narrowing the overall medial-to-lateral dimension of the roof-forming array. (2) Movements and shape changes of the floor cells may also contribute to the narrowing of the

Fig. 8. Morphology of the roof and floor cells is severely disrupted in stage 13 *bullwinkle* egg chambers. Optical projections showing lateral views of wild-type (A–C) and dorsolateral views of a *bwk* egg chamber (E–G). Dorsal midlines are indicated by white lines, with anterior at the top left corner. In wild type, the roof-forming (A, outlined in blue) and floor-forming populations (B) are wider over the anterior, paddle region and narrower over the stalk. (E–F) In *bwk*, however, the roof population does not extend as far anteriorly; it is also bifurcated (arrow, E), consistent with the splitting of the floor-forming population evident in F (arrow). (C, G) Merges of the projections of A and B, and E and F, respectively. In C, the base of the dorsal appendage is out of the picture, to the bottom right. In G, high-Broad roof cells (blue) have advanced anterior (arrowheads) of the floor cells (red). (D, H) Dorsal appendage morphology of wild-type (D) and bwk^{151}/bwk^{8482} eggshells (H) from different egg chambers than those shown above. Wild-type (D) dorsal appendages, shown in a lateral view, have a long narrow stalk and a flattened paddle (see also Fig. 1F). (H) A dorsolateral view of a *bwk* egg chamber shows two appendages; the upper one continues out of the plane of focus. In *bwk*, the dorsal appendages are short, wide, and irregular.

roof population array. The angled protrusion of anterior row floor cells toward the midline may pull the attached roof cells medially. (3) Finally, rearrangement of roof cells in the plane of the epithelium may contribute to the narrowing or lengthening of the array. Such intercalation of cells in one direction (convergence) is a highly conserved mechanism

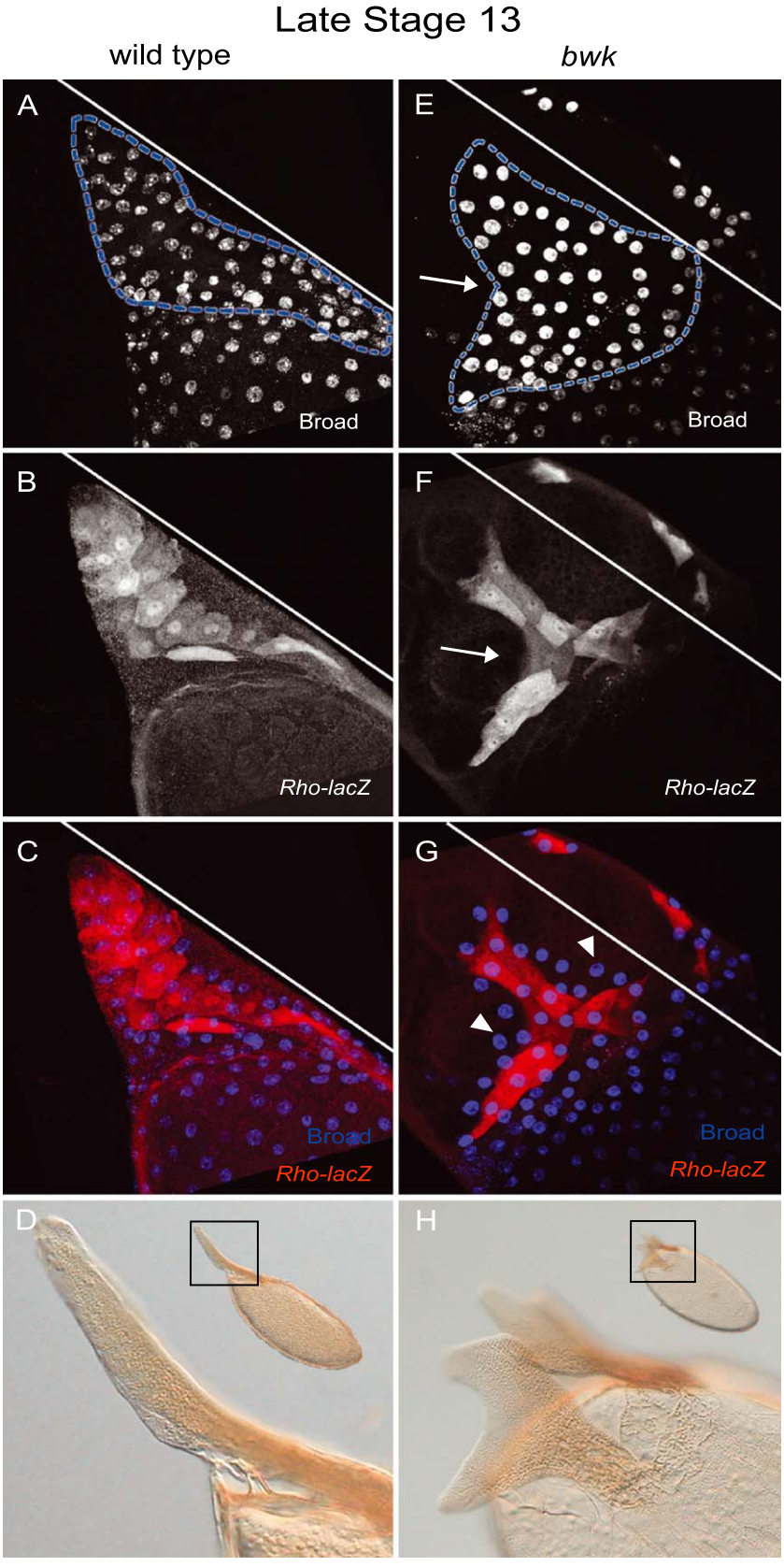

Table 1
Morphological and molecular characteristics of roof and floor cells in a single dorsal appendage primordium

Number of cells	Markers expressed	Initial position	Cell shape changes
Roof cells			
50–60 per appendage	High Broad No *rho-lacZ*	Immediately posterior and lateral of floor-forming cells	Stage 10B: early elongation; late stage 10B-12: apical constriction; stage 13: apical expansion
Floor cells			
11–15 per appendage	No Broad High *rho-lacZ*	Posterior to centripetal cells and lateral of dorsal midline in 'Γ'-shaped 'hinge'	Stage 10B: early elongation; early stage 11: basal constriction, trapezoidal apices, nuclei descend; stages 11–12: late elongation; stage 13: shortening

that produces elongation (extension) of epithelial tissues in both vertebrate and invertebrate embryos (Cooper and Kimmel, 1998; Irvine and Wieschaus, 1994; Keller, 2002; Lengyel and Iwaki, 2002).

Since we have not marked and followed individual cells throughout dorsal appendage formation, we cannot be certain that the dorsal-appendage-forming cells rearrange (i.e., exchange nearest neighbors) in the plane of the epithelium. Nonetheless, our work has produced indirect evidence suggesting that cell rearrangement plays a role in dorsal appendage formation. While the total number of apically constricted cells is the same in early stage 11 and early stage 12, the configuration of cells changes in a manner consistent with rearrangement. In early stage 11, the apically constricted array is nine cells long (from anterior to posterior) at the longest point, while in early stage 12 it is longer (13 cells long at the longest point; Figs. 2K vs. N, 54 and 55 apically constricted cells, respectively). Interestingly, dorsal appendage formation in *D. virilis* also involves the apical constriction and possible rearrangement of high-Broad roof cells (James and Berg, 2003).

Directed cell elongation forms the floor

Once morphogenesis begins, the *rhomboid-lacZ* marker specifically identifies the floor cells, offering an unprecedented view of floor formation. The floor cells undergo three distinct periods of cell-shape change: (1) early elongation in stage 10B, (2) late elongation during stages 11 and 12, and (3) cell shortening in stage 13.

Late floor cell elongation bears certain morphological resemblances to *Drosophila* embryonic dorsal closure, which has been likened to wound healing in vertebrates (Harden, 2002; Jacinto et al., 2001; Kiehart et al., 2000; Ramet et al., 2002; Wood et al., 2002). During dorsal closure, a gap in the ectoderm is sealed as two sheets of epithelial cells elongate from the left and right sides of the embryo towards the dorsal midline where they fuse (Harden, 2002). Likewise, during dorsal appendage formation, floor cells from the anterior and medial rows elongate toward each other until they meet and seal. Both processes entail the directed elongation of a group of cells upon a second group of apically constricted cells; in both contexts, two cell-fronts advance until they meet to form a continuous layer. Future studies will determine if these morphological parallels are borne out by molecular parallels.

Another outstanding question is what causes the *rho-lacZ* cells to undergo the dramatic movements and cell-shape changes that form the floor? The cytoskeletal alterations necessary for elongation may be regulated by the Rho, Rac, and Cdc42 family of GTPases or by their effectors, such as Rho Kinase 2, which is required for cell elongation during vertebrate gastrulation (Marlow et al., 2002). During dorsal closure, the small GTPases serve as upstream activators of the JNK pathway, which is in turn essential for elongation of the leading-edge cells (Harden, 2002). Fos, one of the most downstream components of the JNK pathway, is necessary for elongation during dorsal closure (Reed et al., 2001; Riesgo-Escovar and Hafen, 1997) and is also required during dorsal appendage morphogenesis (Dequier et al., 2001). The timing of Fos expression appears consistent with a role in floor cell elongation (data not shown), but future studies are necessary to determine whether floor cell elongation requires Fos.

Coordination between roof and floor cells

The roof- and floor-forming cells display distinct morphologies, behaviors, and molecular profiles, yet their actions must be intimately coordinated throughout morphogenesis to form and lengthen an intact tube. During stage 11, for example, many cell shape-changes and movements must be coordinated to transform the flat single-layered epithelium into a nascent tube. During this rapid transformation, features of roof and floor formation are subtly graded from anterior-to-posterior and/or from medial-to-lateral, including apical constriction and floor cell elongation. The secretion of a morphogen affecting both roof and floor cell gene expression is one appealing mechanism by which coordination of the two populations could be achieved.

Another phase of morphogenesis requiring coordination of roof and floor cells is anterior extension. During this process, both cell populations must move forward, and eventually arrest, in concert. Although we have not established which population is driving this anterior movement, the high-Broad roof cells may actively migrate on the basal lamina ensheathing each egg chamber, pulling the floor cells forward passively, as in epiboly during vertebrate gastrulation. This possibility seems likely since in stage 13 *bullwinkle* mutants, high-Broad cells appear able to advance despite compromised *rho-lacZ* cell movement (arrowheads, Fig.

8G). Furthermore, the roof cells of cultured egg chambers extend filopodia (data not shown), suggesting an active movement. Nonetheless, it is also possible that the required force could be generated at the rear of the epithelium by convergent-extension or that floor cells contribute to anterior movement. Studies that disrupt cytoskeletal or adhesion functions in small clones of follicle cells may clarify whether one or both subpopulations are actively motile during dorsal appendage formation.

bullwinkle disrupts both roof and floor morphogenesis

Although each subpopulation appears correctly fated in the *bwk* mutant and the initial events of morphogenesis occur normally, both roof and floor cells display later abnormalities. Why might roof formation be defective in *bwk*? *bwk* roof cells reduce their apical size normally throughout stage 11, so their unusually wide arrays do not result from a defect in this shape change. If intercalation drives anterior extension, then a defect in this process might explain the shorter and wider dorsal appendages of the mutant. Alternatively, defects in floor cell movement could potentially impair roof formation, as the two populations remain moored to each other throughout morphogenesis. In wild type, the lateral-most *rho-lacZ* cells elongate towards the midline and may pull the attached roof cells in that direction, thereby exerting a force that narrows the mediolateral extent of the array. In *bwk* mutants, however, the lateral-most *rho-lacZ* cells often fail to project towards the midline; instead, they jut out to the side. The persistent lateral presence of these cells may hinder the medial movement of the attached roof cells. Only by developing methods to specifically block movement of either the roof or the floor-forming populations will it be possible to assess their relative contributions to active motility.

In addition to the above positional defects, *rhomboid-lacZ* cells often fail to form a cohesive floor and detach from each other along their lateral surfaces. The observed floor cell phenotypes are consistent with an adhesion defect, resulting either from insufficient adhesion between floor cells or from their excessive adhesion to the substrate. For example, the frequent failure of anterior- and medial-row *rho-lacZ* cells to seal into a continuous floor may represent a failure to establish the adhesive contacts that stabilize epithelial fusion events (Martin and Wood, 2002). Our culture studies also support the presence of adhesion defects in *bwk* egg chambers: *bwk* follicle cells round up and delaminate and the integrity of the follicular epithelium appears generally compromised. Although the distribution of E-cadherin is normal in *bwk* egg chambers, other molecules governing cell-substrate adhesion may be misregulated in *bwk* egg chambers, including integrins, FasIII, or other cadherins.

Mutations in *bullwinkle* affect other processes, including follicle-cell shape change and movement. How might this single gene impinge upon all these phenomena? Because the *bwk* gene product is a putative transcription factor and is required in the germline for the proper morphogenesis of the overlying somatic follicle cells, it likely influences these processes by regulating a signal between the two cell types (Rittenhouse and Berg, 1995). Altering this signal in the mutant could disrupt extracellular matrix composition, compromise focal-adhesion-kinase or integrin function, or modify cytoskeletal organization, preventing the adhesive and cytoskeletal changes necessary for morphogenesis. Although the nature of the germline-to-soma signal remains elusive, genetic studies demonstrate that the *bullwinkle* dorsal appendage phenotype can be enhanced and suppressed by interacting genes that function in the somatic follicle cells (Tran and Berg, 2003). This result, together with our analysis of the morphogenetic process, highlights the intimate cooperation between adjacent tissue layers that is necessary for complex morphogenesis.

Dorsal appendage formation, in its relative simplicity, nonetheless offers a rich array of cell shape-changes and movements that can be imaged in living specimens and dissected with genetic tools. As such, it represents an excellent arena in which to investigate epithelial morphogenesis as well as an important opportunity for elucidating how different organisms build dramatically distinct body plans with similar genetic building blocks.

Acknowledgments

Thanks to Tadashi Uemura, Hiroki Oda, Greg Guild, and Hannele Ruohola-Baker for antibodies; Tony Ip, Hannele Ruohola-Baker, and Trudi Schüpbach for flies; Marianne Bronner-Fraser and Kai Zinn for lab space and encouragement; and Paulette Brunner, Andy Ewald, and Steve Potter for microscopy help. Thanks to Dave Ehlert, Jake Dorman, and Mark Terayama for heroic help creating Figure 1. Thanks to Ellen Ward for sharing unpublished data and, concerning Figure 1, for suggesting that we hire an illustrator who perfected the drawings. Thanks to Dave Tran for the *bwk* image in Figure 8H and to members of the Berg lab for constructive criticism of this manuscript. This work was supported by National Institutes of Health grant RO1-GM-45248 and National Science Foundation grant IBN-9983207 to C.A.B., the Beckman Institute and N.I.H. grant HD37105 to S.E.F., and N.I.H. grant GM33830 to D.P.K. J.B.D. also was supported by the Molecular and Cellular Biology and A.R.C.S. programs at the University of Washington and a Howard Hughes Medical Institute Predoctoral Fellowship.

References

Ainsworth, C., Wan, S., Skaer, H., 2000. Coordinating cell fate and morphogenesis in *Drosophila* renal tubules. Philos. Trans. R. Soc. Lond., B Biol. Sci. 355, 931–937.

Bang, A.G., Kintner, C., 2000. Rhomboid and Star facilitate presentation

and processing of the *Drosophila* TGF-α homolog Spitz. Genes Dev. 14, 177–186.

Bard, J.B., Ross, A.S., 1982. The morphogenesis of the ciliary body of the avian eye: II. Differential enlargement causes an epithelium to form radial folds. Dev. Biol. 92, 87–96.

Bloor, J.W., Kiehart, D.P., 2001. *zipper* Nonmuscle myosin-II functions downstream of PS2 integrin in *Drosophila* myogenesis and is necessary for myofibril formation. Dev. Biol. 239, 215–228.

Colas, J.F., Schoenwolf, G.C., 2001. Towards a cellular and molecular understanding of neurulation. Dev. Dyn. 221, 117–145.

Cooper, M.S., Kimmel, C.B., 1998. Morphogenetic cell behaviors and specification of cell fate during early teleost development. In: Soll, D., Wessels, D. (Eds.), Motion Analysis of Living Cells. Wiley, New York, New York, pp. 177–220.

Costa, M., Sweeton, D., Wieschaus, E., 1993. Gastrulation in *Drosophila*: cellular mechanisms of morphogenesis. In: Bate, M., Martinez-Arias, A. (Eds.), The Development of *Drosophila melanogaster*. Cold Spring Harbor Laboratory Press, Cold Spring Harbor, pp. 425–465.

Costa, M., Wilson, E.T., Wieschaus, E., 1994. A putative cell signal encoded by the *folded gastrulation* gene coordinates cell shape changes during *Drosophila* gastrulation. Cell 76, 1075–1089.

Davidson, L.A., Keller, R.E., 1999. Neural tube closure in *Xenopus laevis* involves medial migration, directed protrusive activity, cell intercalation and convergent extension. Development 126, 4547–4556.

Deng, W.M., Bownes, M., 1997. Two signalling pathways specify localised expression of the *Broad-Complex* in *Drosophila* eggshell patterning and morphogenesis. Development 124, 4639–4647.

Dequier, E., Souid, S., Pal, M., Maroy, P., Lepesant, J.A., Yanicostas, C., 2001. Top-DER- and Dpp-dependent requirements for the *Drosophila fos/kayak* gene in follicular epithelium morphogenesis. Mech. Dev. 106, 47–60.

Dobens, L.L., Raftery, L.A., 2000. Integration of epithelial patterning and morphogenesis in *Drosophila* ovarian follicle cells. Dev. Dyn. 218, 80–93.

Dobens, L.L., Martin-Blanco, E., Martinez-Arias, A., Kafatos, F.C., Raftery, L.A., 2001. *Drosophila puckered* regulates Fos/Jun levels during follicle cell morphogenesis. Development 128, 1845–1856.

Duffy, J.B., Harrison, D.A., Perrimon, N., 1998. Identifying loci required for follicular patterning using directed mosaics. Development 125, 2263–2271.

Dutta, D., Bloor, J.W., Ruiz-Gomez, M., VijayRaghavan, K., Kiehart, D.P., 2002. Real-time imaging of morphogenetic movements in *Drosophila* using Gal4-UAS-driven expression of GFP fused to the actin-binding domain of Moesin. Genesis 34, 146–151.

Edwards, K.A., Kiehart, D.P., 1996. *Drosophila* nonmuscle myosin II has multiple essential roles in imaginal disc and egg chamber morphogenesis. Development 122, 1499–1511.

Edwards, K., Demsky, M., Montague, R., Weymouth, N., Kiehart, D., 1997. GFP-Moesin illuminates actin cytoskeleton dynamics in living tissue and demonstrates cell shape changes during morphogenesis in *Drosophila*. Dev. Biol. 191, 103–117.

Emery, I.F., Bedian, V., Guild, G.M., 1994. Differential expression of *Broad-complex* transcription factors may forecast tissue-specific developmental fates during *Drosophila* metamorphosis. Development 120, 3275–3287.

French, R.L., Cosand, K.A., Berg, C.A., 2003. The *Drosophila* female sterile mutation *twin peaks* is a novel allele of *tramtrack* and reveals a requirement for Ttk69 in epithelial morphogenesis. Dev. Biol. 253, 18–35.

Fristrom, D., 1988. The cellular basis of epithelial morphogenesis. A review. Tissue Cell 20, 645–690.

Harden, N., 2002. Signaling pathways directing the movement and fusion of epithelial sheets: lessons from dorsal closure in *Drosophila*. Differentiation 70, 181–203.

Hardin, J., Keller, R., 1988. The behaviour and function of bottle cells during gastrulation of *Xenopus laevis*. Development 103, 211–230.

Hinton, H.E., 1969. Respiratory systems of insect egg shells. Annu. Rev. Entomol. 14, 343–368.

Hogan, B.L., Kolodziej, P.A., 2002. Organogenesis: molecular mechanisms of tubulogenesis. Nat. Rev. Genet. 3, 513–523.

Hu, N., Castelli-Gair, J., 1999. Study of the posterior spiracles of *Drosophila* as a model to understand the genetic and cellular mechanisms controlling morphogenesis. Dev. Biol. 214, 197–210.

Ip, Y.T., Park, R.E., Kosman, D., Bier, E., Levine, M., 1992. The dorsal gradient morphogen regulates stripes of *rhomboid* expression in the presumptive neuroectoderm of the *Drosophila* embryo. Genes Dev. 6, 1728–1739.

Irvine, K.D., Wieschaus, E., 1994. Cell intercalation during *Drosophila* germband extension and its regulation by pair-rule segmentation genes. Development 120, 827–841.

Jacinto, A., Martinez-Arias, A., Martin, P., 2001. Mechanisms of epithelial fusion and repair. Nat. Cell Biol. 3, E117–E123.

Jackson, S.M., Berg, C.A., 1999. Soma-to-germline interactions during *Drosophila* oogenesis are influenced by dose-sensitive interactions between *cut* and the genes *cappuccino, ovarian tumor* and *agnostic*. Genetics 153, 289–303.

James, K.E., Berg, C.A., 2003. Temporal comparison of Broad-Complex expression during eggshell-appendage patterning and morphogenesis in two *Drosophila* species with different eggshell-appendage numbers. Mechanisms of DevelopmentGene Expr. Patterns 3, 629–634.

James, K.E., Dorman, J.B., Berg, C.A., 2002. Mosaic analyses reveal the function of *Drosophila Ras* in embryonic dorsoventral patterning and dorsal follicle cell morphogenesis. Development 129, 2209–2222.

Keller, R., 2002. Shaping the vertebrate body plan by polarized embryonic cell movements. Science 298, 1950–1954.

Kiehart, D.P., Montague, R.A., Rickoll, W.L., Foard, D., Thomas, G.H., 1994. High-resolution microscopic methods for the analysis of cellular movements in *Drosophila* embryos. Methods Cell Biol. 44, 507–532.

Kiehart, D.P., Galbraith, C.G., Edwards, K.A., Rickoll, W.L., Montague, R.A., 2000. Multiple forces contribute to cell sheet morphogenesis for dorsal closure in *Drosophila*. J. Cell Biol. 149, 471–490.

Kimberly, E.L., Hardin, J., 1998. Bottle cells are required for the initiation of primary invagination in the sea urchin embryo. Dev. Biol. 204, 235–250.

King, R.C., 1970. Ovarian Development in *Drosophila melanogaster*. Academic Press, New York.

King, R., Koch, E., 1963. Studies on ovarian follicle cells of *Drosophila*. Q. J. Microsc. Sci. 104, 297–320.

King, R.C., Vanoucek, E.G., 1960. Oogenesis in adult *Drosophila melanogaster*: X. Studies on the behavior of the follicle cells. Growth 24, 333–338.

Kolega, J., 1986. The cellular basis of epithelial morphogenesis. Dev. Biol. 2, 103–143.

Lee, J.R., Urban, S., Garvey, C.F., Freeman, M., 2001. Regulated intracellular ligand transport and proteolysis control EGF signal activation in *Drosophila*. Cell 107, 161–171.

Lengyel, J.A., Iwaki, D.D., 2002. It takes guts: the *Drosophila* hindgut as a model system for organogenesis. Dev. Biol. 243, 1–19.

Leptin, M., 1999. Gastrulation in *Drosophila*: the logic and the cellular mechanisms. EMBO J. 18, 3187–3192.

Leptin, M., Casal, J., Grunewald, B., Reuter, R., 1992. Mechanisms of early *Drosophila* mesoderm formation. Dev., Suppl., 23–31.

Lubarsky, B., Krasnow, M.A., 2003. Tube morphogenesis: making and shaping biological tubes. Cell 112, 19–28.

Mahajan-Miklos, S., Cooley, L., 1994a. Intercellular cytoplasm transport during *Drosophila* oogenesis. Dev. Biol. 165, 336–351.

Mahajan-Miklos, S., Cooley, L., 1994b. The villin-like protein encoded by the *Drosophila quail* gene is required for actin bundle assembly during oogenesis. Cell 78, 291–301.

Manseau, L., Calley, J., Phan, H., 1996. Profilin is required for posterior patterning of the *Drosophila* oocyte. Development 122, 2109–2116.

Margaritis, L.H., 1984. Microtubules during formation of the micropylar canal in *Drosophila melanogaster*. Cell Biol. Int. Rep. 8, 317–321.

Margaritis, L.H., Kafatos, F.C., Petri, W.H., 1980. The eggshell of *Droso-*

phila melanogaster: I. Fine structure of the layers and regions of the wild-type eggshell. J. Cell. Sci. 43, 1–35.
Margolis, J., Spradling, A., 1995. Identification and behavior of epithelial stem cells in the *Drosophila* ovary. Development 121, 3797–3807.
Marlow, F., Topczewski, J., Sepich, D., Solnica-Krezel, L., 2002. Zebrafish Rho kinase 2 acts downstream of Wnt11 to mediate cell polarity and effective convergence and extension movements. Curr. Biol. 12, 876–884.
Martin, P., Wood, W., 2002. Epithelial fusions in the embryo. Curr. Opin. Cell Biol. 14, 569–574.
Montell, D.J., Rørth, P., Spradling, A.C., 1992. *slow border cells*, a locus required for a developmentally regulated cell migration during oogenesis, encodes *Drosophila* C/EBP. Cell 71, 51–62.
Myat, M.M., Andrew, D.J., 2000. Organ shape in the *Drosophila* salivary gland is controlled by regulated, sequential internalization of the primordia. Development 127, 679–691.
Nezis, I.P., Stravopodis, D.J., Papassideri, I., Robert-Nicoud, M., Margaritis, L.H., 2002. Dynamics of apoptosis in the ovarian follicle cells during the late stages of *Drosophila* oogenesis. Cell Tissue Res. 307, 401–409.
Niewiadomska, P., Godt, D., Tepass, U., 1999. DE-Cadherin is required for intercellular motility during *Drosophila* oogenesis. J. Cell Biol. 144, 533–547.
Nilson, L.A., Schüpbach, T., 1999. EGF receptor signaling in *Drosophila* oogenesis. Curr. Top. Dev. Biol. 44, 203–243.
Oda, H., Uemura, T., Harada, Y., Iwai, Y., Takeichi, M., 1994. A *Drosophila* homolog of Cadherin associated with Armadillo and essential for embryonic cell–cell adhesion. Dev. Biol. 165, 716–726.
Peri, F., Roth, S., 2000. Combined activities of Gurken and Decapentaplegic specify dorsal chorion structures of the *Drosophila* egg. Development 127, 841–850.
Petri, W., Mindrinos, M., Lombard, M., Margaritis, L., 1979. In vitro development of the *Drosophila* chorion in a chemically defined organ culture medium. Wilhelm Roux' Arch. 186, 351–362.
Peri, F., Bokel, C., Roth, S., 1999. Local Gurken signaling and dynamic MAPK activation during *Drosophila* oogenesis. Mech. Dev. 81, 75–88.
Queenan, A.M., Ghabrial, A., Schüpbach, T., 1997. Ectopic activation of *torpedo/Egfr*, a *Drosophila* receptor tyrosine kinase, dorsalizes both the eggshell and the embryo. Development 124, 3871–3880.
Ramet, M., Lanot, R., Zachary, D., Manfruelli, P., 2002. JNK signaling pathway is required for efficient wound healing in *Drosophila*. Dev. Biol. 241, 145–156.
Reed, B.H., Wilk, R., Lipshitz, H.D., 2001. Downregulation of Jun kinase signaling in the amnioserosa is essential for dorsal closure of the *Drosophila* embryo. Curr. Biol. 11, 1098–1108.
Riesgo-Escovar, J.R., Hafen, E., 1997. Common and distinct roles of DFos and DJun during *Drosophila* development. Science 278, 669–672.
Rittenhouse, K., 1996. Bullwinkle, an HMG box protein, is required for proper development during oogenesis, embryogenesis, and metamorphosis in *Drosophila melanogaster*. Dissertation, Department of Genetics, University of Washington, Seattle.
Rittenhouse, K.R., Berg, C.A., 1995. Mutations in the *Drosophila* gene *bullwinkle* cause the formation of abnormal eggshell structures and bicaudal embryos. Development 121, 3023–3033.
Robb, J., 1969. Maintenance of imaginal discs of *Drosophila melanogaster* in chemically defined media. J. Cell Biol. 41, 876–885.
Ruohola-Baker, H., Grell, E., Chou, T.-B., Baker, D., Jan, L.Y., Jan, Y.N., 1993. Spatially localized *rhomboid* is required for establishment of the dorsal-ventral axis in *Drosophila* oogenesis. Cell 73, 953–965.
Sapir, A., Schweitzer, R., Shilo, B.Z., 1998. Sequential activation of the EGF receptor pathway during *Drosophila oogenesis* establishes the dorsoventral axis. Development 125, 191–200.
Schiff, P.E., D'Agostino, R.B., 1996. Practical Engineering Statistics. Wiley, New York.
Schöck, F., Perrimon, N., 2002. Molecular mechanisms of epithelial morphogenesis. Annu. Rev. Cell Dev. Biol. 18, 463–493.
Schoenwolf, G.C., Smith, J.L., 2000. Mechanisms of neurulation. Methods Mol. Biol. 136, 125–134.
Shih, J., Keller, R., 1992. Patterns of cell motility in the organizer and dorsal mesoderm of *Xenopus laevis*. Development 116, 915–930.
Smith, J.L., Schoenwolf, G.C., Quan, J., 1994. Quantitative analyses of neuroepithelial cell shapes during bending of the mouse neural plate. J. Comp. Neurol. 342, 144–151.
Spradling, A.C., 1993. Developmental genetics of oogenesis. In: Bate, M., Martinez-Arias, A. (Eds.), The Development of *Drosophila melanogaster*. Cold Spring Harbor Laboratory Press, Cold Spring Harbor, pp. 1–69.
Stevens, L., 1998. Twin peaks: *Spitz* and *Argos* star in patterning of the *Drosophila* egg. Cell 95, 291–294.
Suzanne, M., Perrimon, N., Noselli, S., 2001. The *Drosophila* JNK pathway controls the morphogenesis of the egg dorsal appendages and micropyle. Dev. Biol. 237, 282–294.
Tepass, U., Gruszynski-DeFeo, E., Haag, T.A., Omatyar, L., Torok, T., Hartenstein, V., 1996. *shotgun* encodes *Drosophila* E-cadherin and is preferentially required during cell rearrangement in the neurectoderm and other morphogenetically active epithelia. Genes Dev. 10, 672–685.
Tran, D.H., Berg, C.A., 2003. *bullwinkle* and *shark* regulate dorsal-appendage morphogenesis in *Drosophila* oogenesis. Development 130, 6273–6282.
Twombly, V., Blackman, R., Jin, H., Graff, J., Padgett, R., Gelbart, W., 1996. The TGF-β signaling pathway is essential for *Drosophila* oogenesis. Development 122, 1555–1565.
Tzolovsky, G., Deng, W.M., Schlitt, T., Bownes, M., 1999. The function of the *broad-complex* during *Drosophila melanogaster* oogenesis. Genetics 153, 1371–1383.
Urban, S., Lee, J.R., Freeman, M., 2001. *Drosophila rhomboid-1* defines a family of putative intramembrane serine proteases. Cell 107, 173–182.
Urban, S., Lee, J.R., Freeman, M., 2002. A family of Rhomboid intramembrane proteases activates all *Drosophila* membrane-tethered EGF ligands. EMBO J. 21, 4277–4286.
von Kalm, L., Fristrom, D., Fristrom, J., 1995. The making of a fly leg: a model for epithelial morphogenesis. BioEssays 17, 693–702.
Waring, G.L., 2000. Morphogenesis of the eggshell in *Drosophila*. Int. Rev. Cytol. 198, 67–108.
Wasserman, J.D., Freeman, M., 1998. An autoregulatory cascade of EGF receptor signaling patterns the *Drosophila* egg. Cell 95, 355–364.
Wood, W., Jacinto, A., Grose, R., Woolner, S., Gale, J., Wilson, C., Martin, P., 2002. Wound healing recapitulates morphogenesis in *Drosophila* embryos. Nat. Cell Biol. 4, 907–912.
Young, P.E., Pesacreta, T.C., Kiehart, D.P., 1991. Dynamic changes in the distribution of cytoplasmic myosin during *Drosophila* embryogenesis. Development 111, 1–14.